JCTC Journal of Chemical Theory and Computation

Article

pubs.acs.org/JCTC

Benchmark of Bethe-Salpeter for Triplet Excited-States

Denis Jacquemin,*[,†,‡] Ivan Duchemin,[¶,§] Aymeric Blondel,[†] and Xavier Blase*[,∥,§]

[†]Laboratoire CEISAM - UMR CNR 6230, Université de Nantes, 2 Rue de la Houssinière, BP 92208, 44322 Nantes Cedex 3, France

[‡]Institut Universitaire de France, 103 bd St. Michel, 75005 Paris Cedex 5, France

[¶]INAC, SP2M/L_Sim, CEA/UJF Cedex 09, 38054 Grenoble, France

[§]Institut NEEL, Université Grenoble Alpes, F-38042 Grenoble, France

[∥]CNRS, Institut NEEL, F-38042 Grenoble, France

Supporting Information

ABSTRACT: We have evaluated the accuracy of the Bethe-Salpeter singlet−triplet transition energies as well as singlet−triplet and triplet−triplet splittings for 20 organic molecules, using as reference the CC3 values determined by Thiel and co-workers with both the TZVP and *aug*-cc-pVTZ atomic basis sets. Our excitation energies are obtained on the basis of *GW* quasiparticle energy levels that are self-consistently converged with respect to the starting DFT eigenvalues. In its current form, BSE/*GW* is often unable to provide a balanced description of both singlet and triplet excited-states. While the singlet−singlet and triplet−triplet energy separations are obtained accurately, triplets are located too close in energy from the ground-state, by typically −0.55 eV when using standard functionals to generate the starting eigenstates. Applying the Tamm-Dancoff approximation upshifts the BSE triplet energies and allows reducing this error to ca. −0.40 eV, while using M06-HF eigenstates allows a further increase and hence a reduction of the error for triplet states, but at the cost of larger errors for the singlet excited-states. At this stage, the most accurate TD-DFT estimates therefore remain competitive for computing singlet−triplet transition energies. Indeed, with M06-2X, irrespective of the application or not of the Tamm-Dancoff approximation and of the selected atomic basis set, the deviations obtained with TD-DFT are rather small.

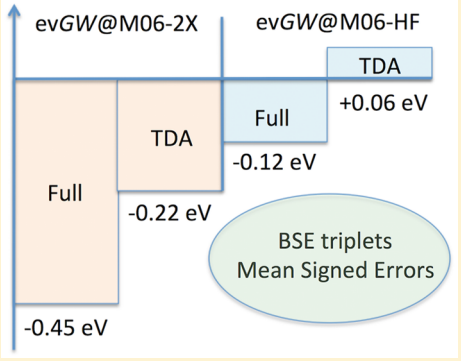

1. INTRODUCTION

Improving the electron-photon interconversion rates is the key to many applications in organic electronics.[1] To this end, the nature of the relevant electronic excited-states (ES) and of the related photophysical phenomena have to be rationalized and controlled. Recently several complex photophysical processes, e.g., thermally activated delayed fluorescence (TADF),[2] singlet fission (SF),[3] and triplet−triplet annihilation (TTA),[4] have attracted considerable attention in both light-to-electricity (solar cells) and electricity-to-light (emitting diodes) fields. TADF derivatives take advantage of an efficient reverse intersystem crossing from a triplet ES to a singlet ES, allowing harvesting triplet excitons and hence increasing the conversion rates of emitting materials.[5] SF materials are attractive for solar cells applications since they can be used to build solar cells with external photocurrent quantum efficiencies exceeding 100%.[6] Likewise, TTA compounds, which can generate one singlet ES from two triplets located on neighboring molecules, can provide much improved conversion efficiencies.[7] In all these processes (TADF, TTA, and SF), controlling the singlet−triplet energy separations (typically $\Delta E_{S_0T_1}$ and/or $\Delta E_{S_1T_1}$) is a preliminary condition for efficient applications, that is, $\Delta E_{S_1T_1}$ should be as small as possible for TADF and the lowest triplet should be about halfway between the singlet ground-state (GS) and singlet ES for SF, i.e., $\Delta E_{S_0T_1} \simeq \Delta E_{S_1T_1} \simeq \frac{1}{2}\Delta E_{S_0S_1}$.

To help drive the organic synthesis toward the most promising molecules, one can rely on first-principle approaches allowing to predict ΔE_{ST}. However, such a task remains extremely challenging. Indeed, Time-Dependent Density Functional Theory (TD-DFT), the most popular method for evaluating ES properties, often yields an unbalanced description of the singlet and triplet ES.[8−15] Indeed, TD-DFT results are highly dependent on the selected exchange-correlation functional (XCF)[9] and are often rather poor for triplet ES.[10,12] Peach and Tozer have thoroughly analyzed the origin of this problem[12] and have shown that, on the one hand, the large TD-DFT errors for singlet−triplet excitation energies are related to the instability of the triplet and, on the other hand, that the TD-DFT errors can be reduced by simultaneously applying the Tamm-Dancoff approximation (TDA), that uncouples the GS and the ES, and selecting an adequate XCF. More recently, Brédas and co-workers[16] and Brückner and Engels[17] obtained accurate TD-DFT ΔE_{ST} for a series of TADF and SF dyes, respectively. However, these successes came at the cost of

Received: November 30, 2016
Published: January 20, 2017

DOI: 10.1021/acs.jctc.6b01169
J. Chem. Theory Comput. 2017, 13, 767−783

tuning the parameters used in the hybrid XCF. Such parametrization can be carried out non-empirically[18] but this implies a non-negligible computational effort. Likewise, the alternative theoretical methods able to provide ΔE_{ST} for "real-life" molecules have their limitations. For instance, the coupled-cluster CC2 approach[19,20] yields a rather balanced description of singlet and triplet ES[21,22] but presents a less favorable scaling with system size than TD-DFT. Likewise, the effective ΔSCF(DFT) approach, that was applied in various flavors,[20,23−26] is often limited to the lowest triplet state.

Another method for evaluating the transition energies, namely the Bethe-Salpeter equation (BSE) approach,[27−30] has been blooming in chemistry in the past few years.[31−67] In this approach, one first determines DFT eigenvalues and eigenvectors with a given XCF and next corrects these eigenstates with the Green's function based *GW* theory,[30,68−70] before calculating the transition energies at the BSE level. Although the *GW* step implies an increased computational cost with respect to TD-DFT, BSE/*GW* advantageously maintains the same $O(N^4)$ formal scaling with system size as TD-DFT. Interestingly, one can in principle resolve self-consistently the *GW* equations, leading possibly to the same results independently of the XCF used in the initial DFT step. However, such a procedure tends to be rather computationally expensive, and many works are applying the so-called G_0W_0 approximation that is a one-shot perturbative *GW* scheme. This choice is however rather unsatisfying as, for organic molecules at the very least, it has been demonstrated that the BSE/G_0W_0 singlet transition energies strongly depend on the DFT starting point.[57,60] Actually the XCF dependence can even be larger for BSE/G_0W_0 than for TD-DFT.[60] As an intermediate between G_0W_0 and fully self-consistent *GW*, one can apply the ev*GW* approach in which initial DFT quasiparticle energies are self-consistently improved while the corresponding Kohn−Sham orbitals are frozen. This approach is computationally effective, and both the BSE/ev*GW* singlet transition energies and oscillator strengths are rather independent of the starting point when a "standard" XCF is applied,[58,60] as well as rather accurate.[58−60,63,65] While there have been a few investigations of triplet ES with BSE/*GW* in periodic systems, e.g., see refs 71−74, there are to the very best of our knowledge only a very few works that have been dedicated to the BSE/*GW* estimations of triplet excitation energies in molecular systems.[34,57,62,75−78] These works either treated tiny molecules, e.g., dihydrogen, methane, and silane,[62,75] or were limited to the BSE/G_0W_0 method.[34,57,76−78] In the largest investigation to date, Bruneval and co-workers used Thiel's set of molecules[79−83] and the TZVP atomic basis set to evaluate the accuracy of $\Delta E_{S_0T_n}$ transition energies obtained with BSE/G_0W_0.[57] Using a diverse panel of starting XCF, they concluded that these transition energies are significantly underestimated, by as much as −1.3 eV (mean signed error, MSE) when starting from G_0W_0@PBE eigenvalues. As expected, a strong correlation with the error on the corresponding G_0W_0 HOMO−LUMO gap was observed, but a large −0.4 eV (MSE) error was nevertheless obtained in the limit of "perfect" HOMO−LUMO gaps.[57] Using the same set of compounds, we go further in the present work by (i) determining BSE/ev*GW* transition energies, in order to decouple as much as possible the problems associated with the BSE formalism with those associated with the calculations of the HOMO−LUMO gap; (ii) using both TZVP and a much larger atomic basis set, namely *aug*-cc-pVTZ; and (iii) evaluating the impact of the TDA approximation on the BSE transition energies. The present work therefore allows answering several questions. Is the previously noted underestimation of BSE/*GW* $\Delta E_{S_0T_1}$ related to the use of G_0W_0? Is the TDA approximation useful to improve the BSE/ev*GW* description of triplet ES? What are the accuracies that can be expected when $\Delta E_{S_0T_n}$, $\Delta E_{S_1T_1}$, and $\Delta E_{T_1T_n}$ are determined at the BSE/ev*GW* level? Is there an effective protocol to obtain accurate splittings with BSE/*GW*? Of course, while the choice of Thiel's set of compounds allows relying on very accurate wave function benchmarks, it also implies limitations on both the size of the molecules treated and the nature of the excited-states, e.g., charge-transfer ES important for many applications are not considered herein.

2. COMPUTATIONAL DETAILS

All *GW* and BSE calculations have been achieved with the FIESTA package[39,84,85] using the MP2/6-31G(d) ground-state geometries given in the works of Thiel.[79] FIESTA provides an implementation of the *GW* and BSE formalisms with atom-centered Gaussian basis functions and takes advantage of both Coulomb-fitting (RI-V) resolution-of-identity and contour deformation techniques for the needed correlation energy integration.[84] Both "full" BSE and the TDA-BSE calculations were performed for all compounds. As noted in the Introduction, we performed the *GW* calculation at the ev*GW* level, that is, we self-consistently converged the occupied/virtual *GW* energy levels while keeping the input Kohn−Sham eigenfunctions frozen. Such a computationally efficient strategy was shown before, for the same set of molecules, to deliver singlet−singlet transitions energies that are only weakly dependent on the DFT starting point.[58] Here, the starting DFT orbitals were determined with NWChem[86] using the four member of Truhlar's M06 XCF family,[87] the *xfine* integration grid, as well as 10^{-7} au and 10^{-6} au convergence thresholds for the total energies and densities, respectively. These four functionals, M06-L, M06, M06-2X, and M06-HF, allow consideration of XCF with very different *exact* exchange ratio: 0%, 27%, 54%, and 100%, respectively. We corrected, at the ev*GW* level, all valence KS levels and twice that number of virtual levels.[88] We applied both the TZVP and the much larger *aug*-cc-pVTZ atomic basis sets (and the corresponding RI auxiliary basis).[89] These basis sets were selected to allow meaningful comparisons with the theoretical best estimates (TBE) provided by Thiel and co-workers,[79,81,82] as they mostly rely on these two same basis sets. These TBE were typically obtained at the CC3 level of theory for $\Delta E_{S_0T_n}$, and we redirect the interested reader to refs 79, 82 and references therein for further details. The BSE/ev*GW* transition energies are rather sensitive to the selected atomic basis set,[60] so that the use of diffuse orbitals are often needed to obtain values close to basis set convergence. In contrast, in some cases, *aug*-cc-pVTZ yields spurious excited-state and strong state mixing, that are generally avoided with the diffuseless TZVP atomic basis set. For comparison purposes, we performed TD-DFT and TDA-TD-DFT (here after denoted TDA-DFT) calculations with the same functional and atomic basis set using the Gaussian09 program.[90] These calculations used the same XCF, improved SCF convergence threshold (1×10^{-8} au) and the so-called *ultrafine* DFT integration grid. Discussions about the functional and basis set dependencies of the TD-DFT singlet−triplet

DOI: 10.1021/acs.jctc.6b01169
J. Chem. Theory Comput. 2017, 13, 767−783

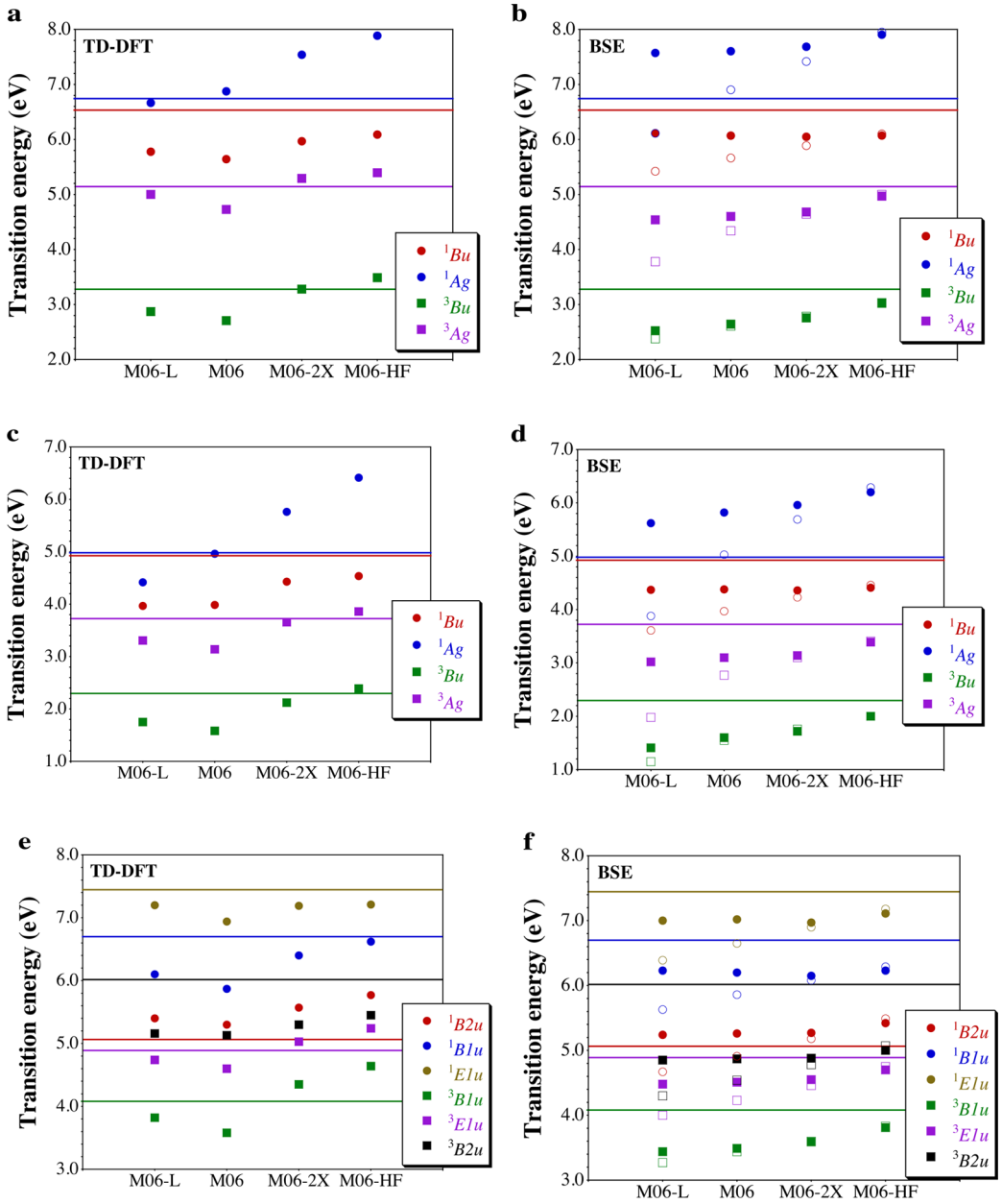

Figure 1. Influence of the selected XCF on the TD-DFT (left) and BSE/*GW* (right) transition energies toward low-lying singlet (circles) and triplet (squares) excited-states of butadiene (a and b), octratetraene (c and d), and benzene (e and f). For the BSE, the closed and open symbols correspond to BSE/ev*GW* and BSE/G_0W_0 results, respectively. All data are obtained with the TZVP basis set. The colored horizontal lines correspond to the CC3/TZVP values of ref 79. Figure S1 in the SI provides the corresponding *aug*-cc-pVTZ results.

energies can already be found in the literature for this set of molecules.[9] We note that M06-2X was generally viewed as an effective XCF for TD-DFT evaluations of singlet−triplet transitions.[9,16] To identify the states corresponding to the TBE ones, we considered the symmetry and the oscillator strengths (for allowed transitions of course) as well as the MO compositions. This allowed for an unambiguous assignment in the vast majority of the cases. Nevertheless, in some cases, e.g., for the 2^1A_1 state of formaldehyde and acetone, two different reasonable assignments could be used (we selected the state with the largest oscillator strength in these cases). As these cases are very limited and mainly present for singlet states, this has no significant impact on the conclusions obtained herein. The interested readers can find comparisons between BSE and TD-DFT computational timings elsewhere.[66] In practice, the additional cost of BSE/ev*GW* compared to TD-DFT is mostly due to the ev*GW* step and not to the BSE part of the calculation. In this framework, we recall that the BSE/ev*GW* computational cost scales as TD-DFT with a $O(N^4)$ dependence, that can be compared to $O(N^5)$, $O(N^6)$, and $O(N^7)$ formal scalings for CC2, CCSD, and CC3, respectively.

3. RESULTS AND DISCUSSION

3.1. Impact of the Selected XCF and of the *GW* Self-Consistency. For five representative molecules, namely, butadiene, octatetraene, benzene, tetrazine, and formaldehyde, we have determined the TD-DFT, BSE/G_0W_0, and BSE/ev*GW* S_0−S_n and S_0−T_n transition energies starting with four different XCF. The G_0W_0 notation means that no self-consistency on the

DOI: 10.1021/acs.jctc.6b01169
J. Chem. Theory Comput. 2017, 13, 767−783

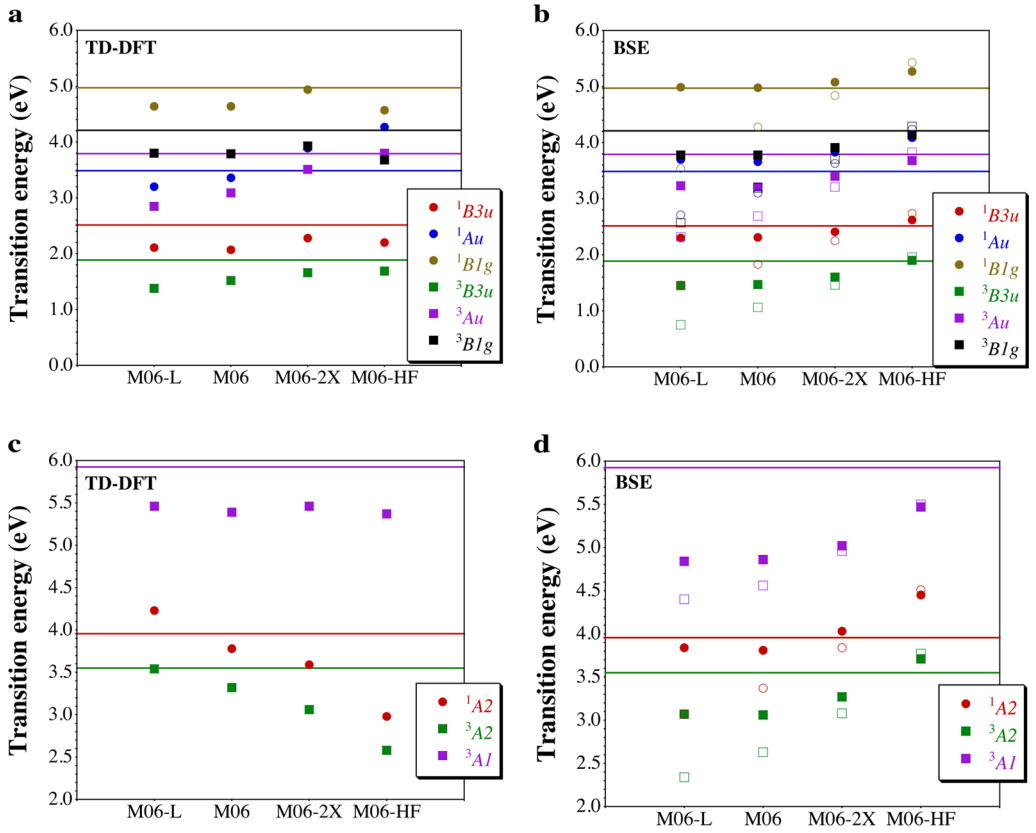

Figure 2. Influence of the selected XCF on the TD-DFT (left) and BSE/*GW* (right) TZVP transition energies of tetrazine (a and b) and formaldehyde (c and d). See the caption of Figure 1 for more details and Figure S2 in the SI for *aug*-cc-pVTZ results.

eigenvalues is performed, namely, the GW formalism is used as a "single-shot" perturbation theory on top of Kohn−Sham eigenstates, leaving a strong dependence on the starting DFT XCF. Our major goal here is to analyze in detail, and for a few systems, the evolution of the singlet and triplet excitation energies as a function of the selected formalism, before providing overall statistics on all molecules in the upcoming Sections. The TZVP results are represented in Figures 1 and 2, whereas the numerical data (including TDA values for all levels of theories) as well as *aug*-cc-pVTZ results can be found in Section S1 of the SI. We recall that for the singlet ES, a comparison of the BSE/ev*GW*@PBE and BSE/ev*GW*@PBE0 transition energies led us to conclude that the impact of the frozen eigenvectors was small, ca. 0.08 eV on average.[58] Here, we go for much more drastic XCF variations as we have in our XCF set both M06-L ("pure" XCF, no *exact* exchange) and M06-HF (full *exact* exchange).

For butadiene (Figures 1a and b), the evolution of the TD-DFT energies with the selected XCF is rather similar for the four states. The ^1B_u state presents a too small energy with the four XCF, and the ^1B_u−^1A_g separation is overestimated, as expected.[91,92] For the ^3B_u and ^3A_g triplet states, all four functionals yield rather reasonable estimates in the TD-DFT framework, M06-2X being the most accurate, which is consistent with the results of ref 9. At the BSE level, let us first notice that the use of G_0W_0 implies a strong dependency from the starting XCF that is very significantly washed out when applying the ev*GW* approach. Obviously, using a pure XCF, M06-L, as a starting point for BSE/G_0W_0 calculations yields far too small transition energies. This outcome, already reported before for singlet ES,[58] holds for triplet ES, e.g., the energy of ^3A_g increases by 1.22 eV when going from BSE/G_0W_0@M06-L to BSE/G_0W_0@M06-HF but only by 0.43 eV when the corresponding ev*GW* eigenstates are used. With BSE/ev*GW*, the M06 and M06-2X transition energies are extremely similar, the M06-L values being also relatively close. With these three XCF, the computed BSE energies of the triplet states are significantly underestimated, in line with a previous report presenting BSE/G_0W_0 results,[57] though clearly the use of ev*GW* improves the estimates. Nevertheless, starting with the M06-HF eigenstates yields slightly larger singlet−triplet transition energies, closer to the CC3 references, illustrating the impact of the frozen eigenfunctions. As can be seen in the SI (Figure S1), all these conclusions hold when the *aug*-cc-pVTZ atomic basis set is used, though, in that case, the upshift induced by the selection of M06-HF is larger. For instance, for the ^3B_u ES, the difference between the BSE/ev*GW*@M06-HF and BSE/ev*GW*@M06-2X *aug*-cc-pVTZ transition energies attains +0.94 eV (Table S6 in the SI), instead of +0.26 eV at the TZVP level (Table S1 in the SI). This effect is related to the presence of intruder states that induce state mixing, e.g., the KS LUMO is an unphysical Rydberg-like orbital with M06-HF/*aug*-cc-pVTZ, while a more physically sound description is reached with the diffuseless basis set or with M06-2X (with the two basis sets). As such, it seems that the BSE/ev*GW* formalism may be more sensitive to the presence of intruder states than TD-DFT.

For octatetraene (Figures 1c and d), the separation between the two lowest singlet ES is obviously hard to reproduce with both TD-DFT and BSE. The BSE/G_0W_0@M06-L approach provides a lucky match for this splitting, but this comes with an underestimation of their absolute energies exceeding 1 eV. The

DOI: 10.1021/acs.jctc.6b01169
J. Chem. Theory Comput. 2017, 13, 767−783

Table 1. Transition Energies from the GS ($\Delta E_{S0}S_n$ and $\Delta E_{S0}T_n$)[a]

			TD-M06-2X		BSE/M06-2X		TD-M06-HF		BSE/M06-HF	
molecule	state	CC3	TDA	full	TDA	full	TDA	full	TDA	full
ethene	$1\ ^1B_{1u}$	8.37	8.42	7.80	8.61	7.84	8.35	7.69	8.54	7.89
	$1\ ^3B_{1u}$	4.48	4.78	4.59	4.17	3.85	4.90	4.67	4.49	4.21
butadiene	$1\ ^1B_u$	6.58	6.47	5.97	6.65	6.05	6.62	6.09	6.60	6.07
	$2\ ^1A_g$	6.77	7.56	7.54	7.71	7.69	8.18	7.89	7.93	7.91
	$1\ ^3B_u$	3.32	3.51	3.28	3.12	2.76	3.75	3.49	3.33	3.02
	$1\ ^3A_g$	5.17	5.41	5.29	4.86	4.68	5.54	5.39	5.14	4.97
hexatriene	$1\ ^1B_u$	5.58	5.38	4.95	5.54	5.04	5.59	5.15	5.51	5.08
	$2\ ^1A_g$	5.72	6.60	6.58	6.77	6.76	7.61	7.19	7.01	6.99
	$1\ ^3B_u$	2.69	2.82	2.56	2.54	2.14	3.11	2.81	2.72	2.39
	$1\ ^3A_g$	4.32	4.50	4.36	4.03	3.82	4.71	4.53	4.24	4.05
octratetraene	$1\ ^1B_u$	4.94	4.67	4.43	4.80	4.36	4.92	4.54	4.80	4.41
	$2\ ^1A_g$	4.97	5.79	5.76	5.99	5.96	6.92	6.41	6.26	6.20
	$1\ ^3B_u$	2.30	2.40	2.12	2.16	1.72	2.71	2.39	2.35	2.00
	$1\ ^3A_g$	3.67	3.82	3.66	3.39	3.14	4.05	3.86	3.60	3.39
cyclopropene	$1\ ^1B_1$	6.90	6.43	6.39	6.76	6.74	6.29	6.17	7.00	6.98
	$1\ ^1B_2$	7.10	6.91	6.55	7.18	6.76	7.09	6.64	7.29	6.90
	$1\ ^3B_2$	4.34	4.51	4.36	4.16	3.90	4.73	4.57	4.42	4.20
	$1\ ^3B_1$	6.62	6.13	6.11	6.24	6.22	6.04	5.96	6.50	6.48
cyclopentadiene	$1\ ^1B_2$	5.73	5.64	5.25	5.66	5.20	5.82	5.37	5.68	5.27
	$2\ ^1A_1$	6.61	7.10	7.07	7.14	7.11	7.74	7.69	7.32	7.29
	$1\ ^3B_2$	3.25	3.43	3.25	2.99	2.70	3.72	3.53	3.18	2.93
	$1\ ^3A_1$	5.09	5.34	5.23	4.86	4.69	5.60	5.47	5.10	4.95
norbornadiene	$1\ ^1A_2$	5.64	5.36	5.15	5.56	5.30	5.54	5.24	5.58	5.35
	$1\ ^1B_2$	6.49	6.12	6.05	6.39	6.31	6.50	6.30	6.49	6.41
	$2\ ^1A_2$	7.64	7.62	7.23	7.86	7.34	7.86	7.46	7.82	7.42
	$2\ ^1A_2$	7.71	7.34	7.20	7.62	7.48	7.43	7.19	7.75	7.65
	$1\ ^3A_2$	3.72	3.80	3.66	3.45	3.22	4.05	3.90	3.72	3.54
	$1\ ^3B_2$	4.16	4.34	4.16	3.92	3.65	4.55	4.35	4.28	4.06
benzene	$1\ ^1B_{2u}$	5.07	5.62	5.57	5.32	5.27	5.89	5.77	5.46	5.42
	$1\ ^1B_{1u}$	6.68	6.65	6.40	6.43	6.15	6.93	6.62	6.46	6.23
	$1\ ^1E_{1u}$	7.45	7.81	7.19	7.65	6.97	7.88	7.21	7.74	7.11
	$1\ ^3B_{1u}$	4.12	4.60	4.35	3.98	3.59	4.97	4.64	4.17	3.81
	$1\ ^3E_{1u}$	4.90	5.05	5.03	4.57	4.55	5.29	5.24	4.73	4.70
	$1\ ^3B_{2u}$	6.04	5.37	5.30	4.94	4.88	5.60	5.45	5.07	5.00
naphthalene	$1\ ^1B_{3u}$	4.27	4.70	4.64	4.45	4.39	4.99	4.86	4.56	4.52
	$1\ ^1B_{2u}$	5.03	4.97	4.73	4.80	4.51	5.40	5.08	4.84	4.61
	$2\ ^1A_g$	5.98	6.58	6.55	6.28	6.23	7.01	6.94	6.42	6.40
	$1\ ^1B_{1g}$	6.07	6.33	6.27	6.11	6.06	6.82	6.54	6.25	6.23
	$2\ ^1B_{3u}$	6.33	6.62	6.11	6.46	5.89	6.75	6.21	6.48	5.97
	$2\ ^1B_{2u}$	6.57	6.83	6.45	6.59	6.17	7.19	5.08	6.65	6.27
	$2\ ^1B_{1g}$	6.79	6.94	6.66	6.76	6.38	7.54	6.54	6.76	6.46
	$3\ ^1A_g$	6.90	7.85	7.67	7.45	7.32	8.61	8.08	7.56	7.44
	$1\ ^3B_{2u}$	3.11	3.36	3.16	2.93	2.61	3.71	3.45	3.07	2.80
	$1\ ^3B_{3u}$	4.18	4.28	4.25	3.90	3.85	4.52	4.47	4.00	3.97
	$1\ ^3B_{1g}$	4.47	4.74	4.62	4.25	4.06	5.00	4.85	4.43	4.27
	$2\ ^3B_{2u}$	4.64	4.90	4.81	4.42	4.32	5.25	5.12	4.53	4.43
	$2\ ^3B_{3u}$	5.11	4.51	4.44	4.19	4.12	4.79	4.61	4.00	4.22
	$1\ ^3A_g$	5.52	5.73	5.70	5.23	5.18	6.01	5.94	5.43	5.39
	$2\ ^3B_{1g}$	6.48	6.35	6.35	6.08	6.07	7.27	7.25	6.21	6.21
	$2\ ^3A_g$	6.47	6.40	6.36	5.99	5.95	6.82	6.74	6.12	6.09
	$3\ ^3A_g$	6.79	7.00	6.95	6.48	6.41	7.89	7.81	6.69	6.64
	$3\ ^3B_{1g}$	6.76	7.20	7.16	6.68	6.61	7.74	7.66	6.97	6.92
furan	$1\ ^1B_2$	6.60	6.77	6.37	6.71	6.26	6.92	6.47	6.75	6.36
	$2\ ^1A_1$	6.62	7.20	7.14	7.00	6.94	7.66	7.54	7.22	7.16
	$3\ ^1A_1$	8.53	9.00	8.40	9.00	8.30	9.07	8.40	9.09	8.44
	$1\ ^3B_2$	4.17	4.38	4.22	3.85	3.58	4.65	4.45	4.11	3.87
	$1\ ^3A_1$	5.48	5.68	5.60	5.15	5.05	5.84	5.70	5.41	5.31
pyrrole	$2\ ^1A_1$	6.40	6.99	6.90	6.73	6.65	7.40	7.27	6.92	6.84
	$1\ ^1B_2$	6.71	6.98	6.62	6.86	6.47	7.17	6.77	6.88	6.55

DOI: 10.1021/acs.jctc.6b01169
J. Chem. Theory Comput. 2017, 13, 767−783

Table 1. continued

molecule	state	CC3	TD-M06-2X		BSE/M06-2X		TD-M06-HF		BSE/M06-HF	
			TDA	full	TDA	full	TDA	full	TDA	full
	$3\ ^1A_1$	8.17	8.66	8.11	8.62	8.00	8.75	8.14	8.70	8.14
	$1\ ^3B_2$	4.48	4.72	4.58	4.17	3.93	5.05	4.87	4.43	4.23
	$1\ ^3A_1$	5.51	5.65	5.59	5.19	5.12	5.86	5.77	5.44	5.37
imidazole	$2\ ^1A'$	6.58	7.05	6.76	6.87	6.57	7.34	6.97	6.99	6.71
	$1\ ^1A''$	6.82	6.60	6.59	6.56	6.55	6.72	6.57	6.79	6.79
	$3\ ^1A'$	7.10	7.56	7.39	7.32	7.12	7.91	7.72	7.45	7.31
	$1\ ^3A'$	4.69	4.91	4.77	4.35	4.12	5.25	5.06	4.61	4.41
	$2\ ^3A'$	5.79	6.00	5.94	5.46	5.36	6.27	5.90	5.79	5.71
	$1\ ^3A''$	6.37	6.14	6.09	6.18	6.15	6.08	6.56	6.58	6.55
	$3\ ^3A'$	6.55	6.43	6.31	5.99	5.87	6.76	6.18	6.29	6.18
pyridine	$1\ ^1B_1$	5.05	4.98	4.88	5.22	5.16	4.98	4.68	5.50	5.46
	$1\ ^1B_2$	5.15	5.76	5.66	5.43	5.35	6.02	5.84	5.56	5.48
	$1\ ^1A_2$	5.50	5.56	5.53	5.52	5.51	6.09	6.00	5.80	5.79
	$2\ ^1A_1$	6.85	6.89	6.61	6.67	6.39	7.16	6.83	6.70	6.45
	$2\ ^1B_2$	7.59	8.01	7.48	7.82	7.25	8.16	7.57	7.92	7.37
	$3\ ^1A_1$	7.70	8.11	7.50	7.95	7.28	8.21	7.54	8.04	7.39
	$1\ ^3A_1$	4.25	4.72	4.46	4.11	3.71	5.08	4.75	4.31	3.95
	$1\ ^3B_1$	4.50	4.31	4.26	4.42	4.39	4.32	4.14	4.78	4.75
	$1\ ^3B_2$	4.86	4.83	4.78	4.34	4.28	5.07	4.96	4.48	4.43
	$2\ ^3A_1$	5.05	5.21	5.17	4.73	4.69	5.47	5.40	4.89	4.85
	$1\ ^3A_2$	5.46	5.46	5.44	5.35	5.33	6.02	5.94	5.64	5.62
	$2\ ^3B_2$	6.40	5.98	5.93	5.51	5.46	6.28	6.17	5.67	5.62
s-tetrazine	$1\ ^1B_{3u}$	2.53	2.45	2.28	2.51	2.41	2.63	2.20	2.70	2.62
	$1\ ^1A_u$	3.79	3.95	3.89	3.86	3.83	4.53	4.27	4.12	4.09
	$1\ ^1B_{1g}$	4.97	5.12	4.94	5.17	5.08	4.97	4.57	5.35	5.27
	$1\ ^1B_{2u}$	5.12	5.96	5.75	5.47	5.27	6.24	5.94	5.60	5.40
	$1\ ^1B_{2g}$	5.34	5.59	5.47	5.58	5.54	5.71	5.31	5.81	5.77
	$2\ ^1A_u$	5.46	5.33	5.23	5.55	5.51	5.73	5.45	5.77	5.72
	$1\ ^3B_{3u}$	1.89	1.72	1.66	1.67	1.60	1.90	1.69	1.90	1.90
	$1\ ^3A_u$	3.52	3.54	3.51	3.43	3.40	3.96	3.80	3.71	3.68
	$1\ ^3B_{1g}$	4.21	3.98	3.93	3.96	3.91	3.85	3.68	4.20	4.14
	$1\ ^3B_{1u}$	4.33	4.79	4.37	4.11	3.64	5.21	4.73	4.31	3.87
	$1\ ^3B_{2u}$	4.54	4.41	4.32	3.82	3.74	4.70	4.55	3.96	3.87
	$1\ ^3B_{2g}$	4.93	4.85	4.79	4.76	4.72	4.93	4.69	5.02	4.97
	$2\ ^3A_u$	5.03	4.88	4.82	4.92	4.88	5.48	5.28	5.17	5.13
	$2\ ^3B_{1u}$	5.38	5.67	5.65	5.01	4.97	5.98	5.92	5.19	5.13
formaldehyde	$1\ ^1A_2$	3.95	3.68	3.59	4.07	4.03	3.31	2.98	4.49	4.45
	$1\ ^1B_1$	9.18	8.80	8.66	9.24	9.17	8.53	8.16	9.60	9.54
	$2\ ^1A_1$	10.45	10.96	10.81	10.98	10.71	9.95	11.38	11.08	10.96
	$1\ ^3A_2$	3.55	3.12	3.06	3.31	3.27	2.81	2.58	3.75	3.71
	$2\ ^3A_1$	5.83	5.82	5.46	5.35	5.02	5.80	5.37	5.75	5.47
acetone	$1\ ^1A_2$	4.40	4.18	4.11	4.47	4.44	3.65	3.36	4.95	4.92
	$2\ ^1B_1$	9.17	8.70	8.59	9.44	9.40	8.45	8.11	9.88	9.84
	$2\ ^1A_1$	9.65	10.01	8.91	10.17	9.83	9.42	8.96	10.39	10.11
	$1\ ^3A_2$	4.05	3.69	3.63	3.81	3.78	3.23	3.00	4.29	4.27
	$1\ ^3A_1$	6.03	5.92	5.61	5.80	5.54	5.98	5.65	6.12	5.90
benzoquinone	$1\ ^1A_u$	2.85	2.94	2.85	3.12	3.09	2.89	2.54	3.46	3.43
	$1\ ^1B_{1g}$	2.75	2.75	2.67	3.02	2.99	2.71	2.38	3.40	3.37
	$1\ ^1B_{3g}$	4.59	4.39	4.25	4.52	4.34	4.95	4.74	4.60	4.41
	$1\ ^1B_{1u}$	5.62	5.60	5.24	5.74	5.29	6.01	5.60	5.73	5.31
	$1\ ^1B_{3u}$	5.82	6.38	6.35	6.34	6.32	7.02	6.88	6.67	6.66
	$2\ ^1B_{3g}$	7.27	7.38	7.23	7.40	7.24	8.03	7.85	7.57	7.42
	$2\ ^1B_{1u}$	7.82	8.25	7.75	8.43	7.89	8.70	8.16	8.49	7.98
	$1\ ^3B_{1g}$	2.51	2.32	2.26	2.47	2.44	2.30	2.06	2.87	2.84
	$1\ ^3A_u$	2.62	2.49	2.42	2.56	2.53	2.46	2.21	2.91	2.88
	$1\ ^3B_{1u}$	2.96	2.92	2.50	2.71	2.34	3.18	2.67	2.87	2.55
	$1\ ^3B_{3g}$	3.41	3.29	3.16	3.04	2.85	3.66	3.50	3.13	2.94
formamide	$1\ ^1A''$	5.65	5.43	5.37	5.70	5.67	5.09	4.85	6.01	5.98
	$2\ ^1A'$	8.27	8.94	8.69	8.93	8.61	9.56	7.68	9.02	8.79

DOI: 10.1021/acs.jctc.6b01169
J. Chem. Theory Comput. 2017, 13, 767−783

Table 1. continued

molecule	state	CC3	TD-M06-2X		BSE/M06-2X		TD-M06-HF		BSE/M06-HF	
			TDA	full	TDA	full	TDA	full	TDA	full
	$1\ ^3A''$	5.36	5.00	4.92	5.11	5.07	4.71	4.48	5.42	5.39
	$1\ ^3A'$	5.74	5.45	5.20	5.20	5.02	5.40	5.08	5.49	5.33
acetamide	$1\ ^1A''$	5.69	5.50	5.43	5.70	5.69	5.09	4.85	6.14	6.11
	$2\ ^1A'$	7.67	8.14	7.64	8.15	7.90	7.97	7.66	8.34	8.11
	$1\ ^3A''$	5.42	5.08	5.01	5.15	5.10	4.73	4.50	5.56	5.53
	$1\ ^3A'$	5.88	5.59	5.37	5.37	5.20	5.51	5.21	5.74	5.59
propanamide	$1\ ^1A''$	5.72	5.53	5.47	5.73	5.71	5.12	4.89	6.27	6.25
	$2\ ^1A'$	7.62	8.06	7.62	8.07	7.85	7.94	7.64	8.30	8.12
	$1\ ^3A''$	5.45	5.12	5.05	5.17	5.14	4.77	4.54	5.70	5.67
	$1\ ^3A'$	5.90	5.61	5.39	5.39	5.24	5.53	5.23	5.84	5.70

[a]All values are in eV and have been obtained with the TZVP basis set. BSE stands for BSE/ev*GW*. The CC3 values are taken from ref 79. We use the same naming conventions for the ES as in Thiel's original papers.

^1A_g state, that presents a significant double excitation character,[79] is very sensitive to the selected XCF at both TD-DFT (1.99 eV variation range between M06-L and M06-HF) and BSE/G_0W_0 (2.41 eV range) levels. This undesirable effect is greatly damped when ev*GW* eigenvalues are selected (0.58 eV range). Overall, the general trends for octatetraene parallel those of butadiene: the triplet ES energies are too small with BSE, though the magnitude of the error is decreased when using BSE/ev*GW*@M06-HF. Again, the combination of the latter method with *aug*-cc-pVTZ yields larger upshifts than with TZVP (middle right panel of Figure S1).

In benzene (Figures 1e and f), the impact of the XCF strongly depends on the considered state with both TD-DFT and BSE/G_0W_0, though the variations are less dramatic than for the ^1A_g ES of butadiene and octatetraene. In contrast, the BSE/ev*GW* singlet and triplet energies determined with M06-L, M06, and M06-2X are extremely close to one another and this holds with the two atomic basis sets (Figures 1f and S1). As for the linear oligoenes discussed above, the BSE/ev*GW*@M06-HF results are upshifted compared to the ones obtained with the three other XCF, an effect again stronger with the more extended atomic basis set. With this large basis, the lowest singlet ES, $^1B_{2u}$, is accurately predicted in three out of four cases with BSE, whereas TD-DFT overshoots its energy with all tested XCF (bottom right panel of Figure S1). For the lowest triplet ES, $^3B_{1u}$, TD-DFT delivers too small values with both M06-L and M06 but too high values with M06-2X and M06-HF, whereas BSE always undershoots the reference values, to a small extent when using M06-HF (that even yields an overestimation with *aug*-cc-pVTZ). The same trends are found for the second triplet ES, $^3E_{1u}$, whereas for the third one, $^3B_{2u}$, all tested methods undershoot the CC3 benchmark by a significant amount.

For tetrazine (Figures 2a and b and S2), the beneficial impact of the ev*GW* scheme is again very clear for the lowest singlet and triplet B_{3u} ES: the XCF dependency is washed out and remains basically similar to its TD-DFT counterpart, whereas BSE/G_0W_0 transitions energies are very sensitive to the starting XCF. The energies of these singlet and triplet B_{3u} ES are too small with all tested methods, at the exception of the BSE/*GW*@M06-HF approach that provides very accurate estimates. However, there is a cost to this success: the energies of the two higher singlet ES are overestimated by this approach. In contrast, M06-2X allows for better estimates of these higher-lying ES in all tested formalisms. Again, qualitatively similar conclusions are reached with the two atomic basis sets.

In formaldehyde (Figures 2c and d and S2), the XCF dependency of TD-DFT and BSE are markedly different. Indeed, the TD-DFT triplet energies significantly decrease when the amount of *exact* exchange increases, whereas the BSE values follow the opposite trend, with an amplitude of variation that is significantly smaller when the ev*GW* scheme is used, even if the selection of M06-HF yields larger transition energies. Consequently, the TD-M06-HF $\Delta E_{S_0T_n}$ are much too small, whereas the BSE/ev*GW*@M06-HF $\Delta E_{S_0T_n}$ are slightly (TZVP) or significantly (*aug*-cc-pVTZ) exceeding the reference values.

In short, as for singlet ES,[57,60] we found that the BSE/G_0W_0 triplet energies tend to be more dependent on the selected XCF than their TD-DFT counterparts, though the magnitude of this dependency is, on average, more limited for the triplet than for the corresponding singlet ES. BSE/ev*GW* triplet energies are much less XCF-dependent, and the data calculated using M06-L, M06, and M06-2X starting eigenstates are often close to one another but significantly too small compared to the theoretical best estimates. This conclusion parallels the one obtained by Bruneval and co-workers with the BSE/G_0W_0 approach,[57] illustrating that the self-consistent ev*GW* process is not sufficient in itself to reach an accurate description of the triplet ES with BSE. In addition, we found that starting with the M06-HF XCF yields significantly larger BSE/ev*GW* triplet energies in the majority of cases, an effect that is particularly large with the diffuse basis set, due to the presence of intruder states leading state mixing. In the following, we consequently proceed considering the full set of compounds systematically using the ev*GW* approach combined with the four starting M06 XCF (TZVP) or both M06-2X and M06-HF (*aug*-cc-pVTZ).

3.2. Analysis by Molecular Families. The TZVP singlet−triplet transition energies obtained for all molecules with TD-DFT and BSE/ev*GW* applying or not the TDA and using the M06-2X and M06-HF XCF are listed in Table 1. We have also determined the singlet−singlet transition energies for the same molecules because the impact on TDA on the BSE transition energies was, to our knowledge, discussed for very specific cases only up to now,[33,78,93,94] though it is commonly used in solid-state works.[95] Notably, several authors showed that TDA-BSE can yield poor results when simulating nanoscale materials.[78,93] The M06-L and M06 results and the *aug*-cc-pVTZ data with M06-2X and M06-HF are listed in Section S3 of the SI. For each method, we have determined more than 120 ES almost equally divided into singlet and triplet cases. We consider here

DOI: 10.1021/acs.jctc.6b01169
J. Chem. Theory Comput. 2017, 13, 767−783

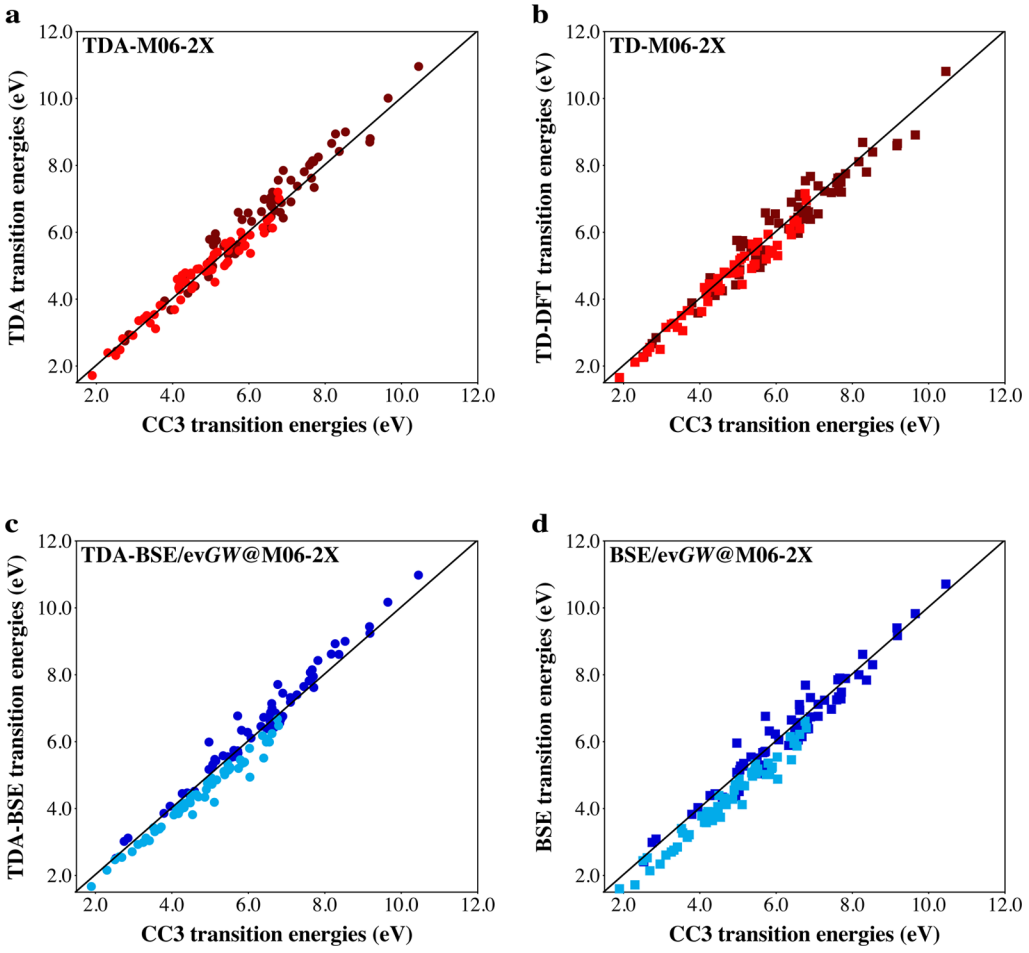

Figure 3. Comparisons between the CC3 and TDA-DFT (a), TD-DFT (b), TDA-BSE (c), and BSE (d) transition energies. The dark- (light-) colored symbols correspond to singlet (triplet) ES, whereas the central line indicates a perfect match with the CC3 values. All values are in eV and have been obtained with the M06-2X XCF and the TZVP atomic basis set.

chemically insightful families of compounds. We mainly focus on the S_0-T_n transition energies and S_1-T_1 splittings as obtained by BSE/ev*GW* and TDA-BSE/ev*GW* using M06-2X and M06-HF eigenstates. Indeed the S_0-S_n cases have already been treated in the literature,[57,58] and the same holds for the TDA-DFT and TD-DFT results.[9,91,92] In addition, as seen above, M06-L or M06 deliver similar results as M06-2X in the BSE/ev*GW* framework.

Unsaturated Aliphatic Hydrocarbons. For ethene, BSE undershoots significantly the energy of the lowest triplet state with M06-2X, an error similar to the one made for the lowest singlet ES, whereas a more accurate triplet result is obtained with M06-HF. TDA increases the BSE energies, resulting in improvements for the two states with both M06-2X and M06-HF. For butadiene, both the ^3B_u and ^3A_g ES are overstabilized by BSE relying on M06-2X or M06-HF eigenstates and the TZVP basis set. Again, TDA improves the description, and the TDA-BSE/ev*GW*@M06-HF results almost perfectly match the CC3 values. BSE provides rather accurate $\Delta E_{S_1T_1}$ in butadiene, whereas this gap tends to be slightly underestimated by all tested TD-DFT variants. For both hexatriene and octatetraene, TDA-BSE and BSE deliver more accurate $\Delta E_{S_1T_1}$ than the corresponding TDA-DFT and TD-DFT methods, but this success originates from too small singlet and triplet ES energies when the "full" BSE scheme is used. Again, TDA upshifts the BSE transition energies, and this effect is significantly smaller for the A_g than for the B_u ES. In cyclopropene, the relative energies of the two triplet ES are nicely estimated (e.g., with M06-2X, $\Delta E_{T_1T_2}$ = 2.32 and 2.09 eV with BSE and TDA-BSE, close to the 2.28 eV reference values), and these ES are again too close to the GS with M06-2X and rather accurate with M06-HF. In cyclopentadiene very similar evolutions with the selected methods are observed. It is noteworthy that applying TDA increases the BSE $^3B_2$ energy by 0.29 eV (0.25 eV) with M06-2X (M06-HF), and that these shifts are slightly larger than their TD-DFT counterparts of 0.18 eV (019 eV). Norbornadiene follows the same trends, that is both M06-2X and M06-HF yield too small BSE $\Delta E_{S_0T_n}$ and $\Delta E_{S_0S_n}$ but quite accurate $\Delta E_{S_1T_1}$ splittings. In contrast, TD-DFT gives too small values for the latter gap, irrespective of the selected XCF. Again, the same trends are observed with *aug*-cc-pVTZ (Table S12) but with exacerbated differences between M06-2X and M06-HF.

Aromatic Hydrocarbons and Heterocycles. Both TDA-BSE and BSE deliver too large transition energies for the $^1B_{2u}$ ES of benzene but too small transition energies for the $^3B_{1u}$ ES, at the notable exception of the TDA-BSE/ev*GW*@M06-HF approach. In all cases, the $\Delta E_{S_1T_1}$ separation remains overshot by more than 0.30 eV. In TD-DFT both singlet and triplet ES are too high, and more accurate S_1-T_1 gaps are consequently reached, especially when applying TDA. For naphthalene, many

DOI: 10.1021/acs.jctc.6b01169
J. Chem. Theory Comput. 2017, 13, 767−783

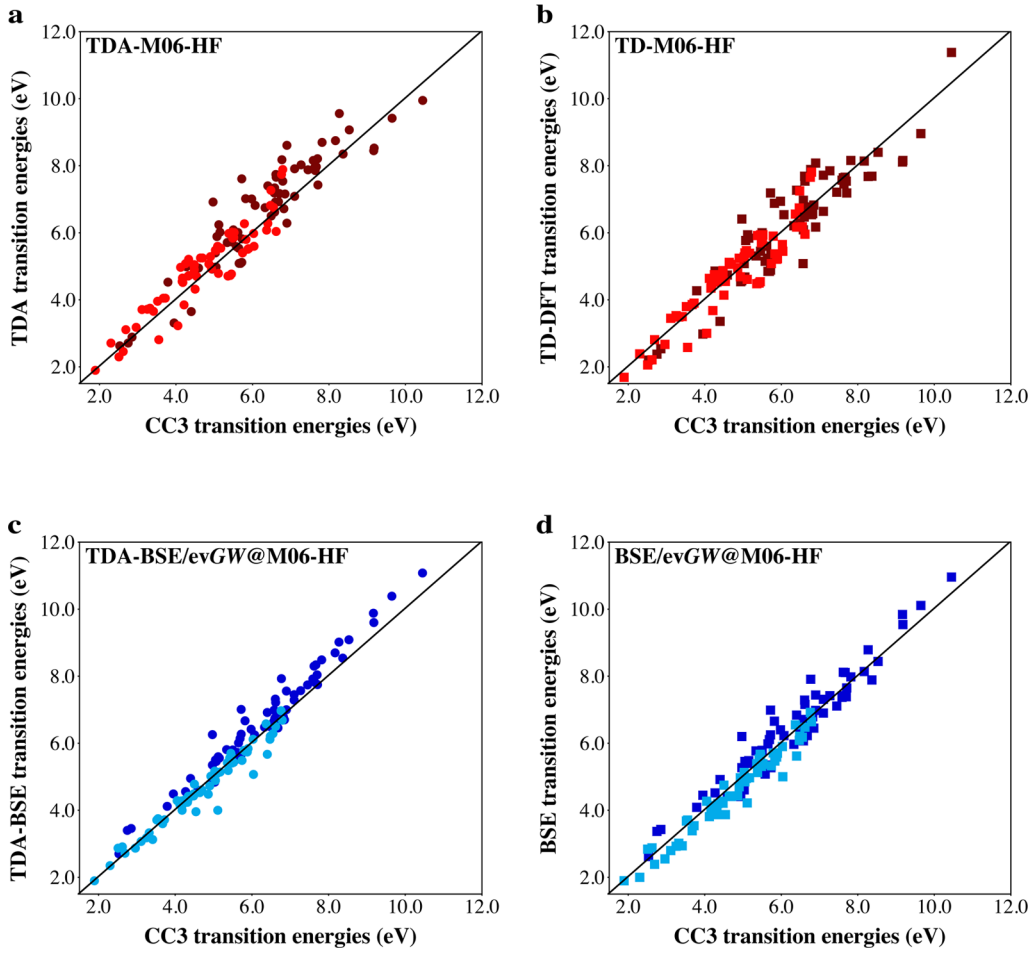

Figure 4. Comparisons between the CC3 and TDA-DFT (a), TD-DFT (b), TDA-BSE (c), and BSE (d) transition energies. All values have been obtained with the M06-HF XCF and the TZVP atomic basis set. See the caption of Figure 3 for more details.

ES have been determined. Interestingly, the mean absolute M06-2X deviations obtained for the triplet ES are 0.25 eV, 0.21 eV, 0.44 eV, and 0.21 eV for TDA-DFT, TD-DFT, TDA-BSE, and BSE, respectively, illustrating that TDA is not a panacea for improving triplet estimates. In fact, the application of TDA systematically increases the transition energies, but this effect ranges from 0.01 eV ($2\ ^3B_{1g}$) to 0.57 eV ($1\ ^1B_{3u}$). Using M06-HF strongly degrades the TDA-DFT (0.61 eV) and TD-DFT (0.54 eV) mean absolute deviations for the triplet ES, whereas the deviations remain reasonably under control with both TDA-BSE (0.25 eV) and BSE (0.29 eV). In furan, all tested theories (but TDA-M06-L) provide too large $\Delta E_{S_1S_2}$ and quite accurate $\Delta E_{T_1T_2}$. BSE delivers reasonably accurate $\Delta E_{S_1T_1}$ splittings with both M06-2X and M06-HF (2.68 and 2.48 eV for a CC3 reference value of 2.43 eV). The outcomes are very similar for pyrrole. For that molecule, considering *aug*-cc-pVTZ, the relative ordering of the $2\ ^1A_1$ and $1\ ^1B_2$ ES differs between CC3 and the TBE (Table S12), and, as expected, all tested TD-DFT and BSE schemes provide the same ranking as CC3. In imidazole, the TZVP TDA-BSE and BSE $\Delta E_{S_1T_1}$ splittings are systematically too large by at least 0.40 eV, whereas BSE/ev*GW*@M06-2X/*aug*-cc-pVTZ provides the most accurate $\Delta E_{S_1T_1}$ among the tested theories (1.65 eV compared to the CC3 reference value of 1.60 eV). This clearly illustrates the uncommon sensitivity to basis set effects of that molecule.[9] For pyridine, none of the selected approaches can accurately predict all key gaps, e.g., BSE largely overestimates $\Delta E_{S_1T_1}$, whereas TD-DFT overshoots the separation between the two lowest singlet ES by at least a factor of 7 (TZVP) or three (*aug*-cc-pVTZ). In tetrazine, as seen above, BSE/ev*GW*@M06-HF gives accurate energies for the lowest ES of the two spin symmetries, and the $\Delta E_{S_1T_1}$ gaps are accurately given by most tested approaches. Again, TDA systematically increases the BSE transition energies, a result holding irrespective of the considered state, basis set, or XCF.

Aldehydes, Ketones, and Amides. In formaldehyde, applying the TDA systematically increases the transition energies, but this effect is only significant for the ES of A_1 symmetry. All methods, but TD-M06-HF, overshoot $\Delta E_{S_1T_1}$, and the error is large with both BSE and TDA-BSE. Unsurprisingly, similar trends are obtained with acetone, for which the energy of the lowest triplet ES (4.05 eV) is underestimated with BSE/ev*GW*@M06-2X (3.78 eV), TD-M06-2X (3.63 eV), and TD-M06-HF (3.00 eV) but overestimated with BSE/ev*GW*@M06-HF (4.27 eV). The same conclusions are obtained with *aug*-cc-pVTZ but with larger variations and absolute errors (see the SI). In benzoquinone, the average variations of the transition energies when applying TDA are +0.18 eV (TD-M06-2X), +0.19 eV (BSE/ev*GW*@M06-2X), +0.31 eV (TD-M06-HF), and +0.17 eV (BSE/ev*GW*@M06-HF), with particularly strong variations for the ES of B_{1u} symmetry. In formamide, acetamide, and propanamide,

DOI: 10.1021/acs.jctc.6b01169
J. Chem. Theory Comput. 2017, 13, 767−783

the reference values for the energies of the lowest triplet ES are very accurately estimated by BSE/ev*GW*@M06-HF, whereas TDA has a relatively small impact. For these three amides, TD-DFT tends to deliver slightly more satisfying $\Delta E_{S_1T_1}$ gaps than BSE.

3.3. Statistical Analysis. Figures 3 and 4 provide comparisons between the TDA-DFT, TD-DFT, TDA-BSE, and BSE transition energies with the CC3/TZVP data for the M06-2X and M06-HF results, respectively (see Section S4 in the SI for M06-L, M06, and *aug*-cc-pVTZ results). In Table 2 we give a statistical analysis for all transitions from the GS to the triplet ES using the CC3 values as references. The corresponding singlet data can be found in Table S13 in the SI, whereas comparisons with TBE can be found in Table S14. The differences between the CC3 and TBE statistics are trifling for triplet ES, as in that case, many TBE are indeed obtained with the CC3 method, whereas larger deviations are found for singlet ES, for which several TBE were obtained with multireference methods, e.g., MR-CI or CAS-PT2.[79,81,82]

Table 2. Statistical Analysis of the Errors of TDA-DFT, TD-DFT, TDA-BSE/ev*GW*, and BSE/ev*GW* Triplet ES Using the Four XCF for the Transition Energies Listed in Tables 1, S11, and S12 Using CC3 Reference Values[a]

method	XCF	MSE	MAE	RMS	Max(+)	Max(−)	*R*
TDA-DFT	M06-L	−0.22	0.26	0.37	0.27	−1.15	0.97
	M06	−0.29	0.30	0.36	0.49	−0.88	0.98
	M06-2X	0.00	0.23	0.27	0.48	−0.67	0.97
		0.00	*0.20*	*0.24*	*0.42*	*−0.79*	*0.98*
	M06-HF	0.20	0.44	0.50	1.10	−0.82	0.93
		0.16	*0.37*	*0.42*	*0.81*	*−0.86*	*0.94*
TD-DFT	M06-L	−0.42	0.42	0.48		−1.16	0.98
	M06	−0.48	0.48	0.51		−0.91	0.99
	M06-2X	−0.12	0.22	0.28	0.40	−0.74	0.98
		−0.13	*0.20*	*0.27*	*0.24*	*−0.79*	*0.98*
	M06-HF	0.01	0.41	0.48	1.02	−1.05	0.93
		−0.06	*0.33*	*0.42*	*0.69*	*−1.00*	*0.94*
TDA-BSE	M06-L	−0.48	0.48	0.51		−1.12	0.99
	M06	−0.42	0.42	0.46		−1.10	0.99
	M06-2X	−0.31	0.31	0.37		−1.10	0.99
		−0.43	*0.43*	*0.48*		*−1.00*	*0.98*
	M06-HF	−0.06	0.17	0.27	0.36	−1.11	0.98
		0.39	*0.46*	*0.52*	*1.45*	*−0.56*	*0.96*
BSE	M06-L	−0.64	0.64	0.67		−1.19	0.99
	M06	−0.58	0.58	0.61		−1.17	0.99
	M06-2X	−0.46	0.46	0.51		−1.16	0.98
		−0.58	*0.58*	*0.63*		*−1.11*	*0.98*
	M06-HF	−0.19	0.27	0.33	0.33	−1.04	0.98
		0.28	*0.37*	*0.46*	*1.45*	*−0.66*	*0.96*

[a]The values in italics correspond to the *aug*-cc-pVTZ data, whereas all other results are obtained with TZVP. MSE, MAE, RMS, Max(+), and Max(−) respectively stand for the mean signed error, mean absolute error, root mean square error, largest positive deviation, and largest negative deviation and are all expressed in eV. *R* is the linear correlation coefficient obtained through a least-square fit. See also Tables S13 and S14 in the SI for singlet ES and comparisons with the TBE for the *aug*-cc-pVTZ values, respectively.

For the transition toward the singlet ES, all BSE/ev*GW* models deliver MSE in the −0.03 to −0.13 eV range and MAE in the 0.26 to 0.29 eV range, except when M06-HF eigenstates are used (Table S13). These values are similar to those reported in ref 58 with the BSE/ev*GW*@PBE0/*aug*-cc-pVTZ model, that is, −0.15 and 0.25 eV, for a similar panel of states,[96] clearly confirming that the ev*GW* procedure washes out the impact of the starting functional when "standard" XCF are used. Indeed, we note that the average differences between TD-PBE0[92] and TD-M06-2X[97] results are twice larger, whereas at the BSE/G_0W_0 level, the quality of the results is strongly dependent on the starting XCF.[57] As the ev*GW* results rely on frozen eigenvectors, using M06-HF to generate the starting solutions yields transition energies significantly differing from their M06-2X counterparts even at the BSE/ev*GW* level. In addition, as can be seen by comparing Figures 4b and d, the estimates obtained with M06-HF for the $\Delta E_{S_0S_n}$ transitions are significantly less dispersed with BSE than with TD-DFT. The correlation coefficient, *R*, obtained on the basis of M06-HF eigenstates is smaller than the corresponding M06-2X values, but this effect is much more marked with TD-DFT. Consequently, we do not recommend the use of BSE/ev*GW*@M06-HF to evaluate singlet ES energies, especially with large basis sets, for which the presence of intruder states is detrimental (see Figure S6 and bottom of Table S13). For the singlet ES, applying TDA upshifts the transition energies for the two theoretical models. Consequently, the small MSE of TD-M06-2X becomes significantly positive with TDA-M06-2X, whereas the negative MSE of BSE/ev*GW*@M06 (underestimation) flips sign when applying TDA (overestimation). Applying the TDA in the BSE/ev*GW* context does not strongly change the MAE obtained for the singlet excited-states but when starting with M06-HF starting eigenstates.

For the triplet excited-states, Figure 3d and Table 2 clearly demonstrate that BSE/ev*GW* provides poor estimates when used in conjunction with M06-2X. Indeed, the MSE is large (−0.46 eV with TZVP, −0.58 eV with *aug*-ccpVTZ), and all $\Delta E_{S0}T_n$ are smaller than their CC3 counterparts. While this result parallels the conclusion obtained by Bruneval and co-workers with the BSE/G_0W_0 approach,[57] where a MSE of (−0.4 eV) was extrapolated in the limit of the "perfect" *GW* HOMO−LUMO gap, it is in sharp contrast with the findings of Rubio's group who studied two porphyrin derivatives and reported an almost perfect match between their BSE/G_0W_0@LDA and experimental triplet energies (deviations of ca. 0.10 eV).[34] As seen above, the use of the partial self-consistent approach in the *GW* step allows the computed triplet energies to be less sensitive to the starting XCF than with G_0W_0. Nevertheless, the dependency on the starting eigenfunctions seems to be slightly larger for the triplet than for the singlet ES (compare the BSE MSE in Tables 2 and S13). Interestingly, using M06-HF/TZVP eigenstates in the BSE calculations allows greatly reducing the error (Figure 4d) with a MSE of −0.19 eV and a MAE of 0.27 eV, successes that come without significant degradation of the correlation with the CC3 values. With the diffuse basis set, one even obtains a positive MSE (see Figure S6), but again, this is probably due to the fortuitous influence of intruder states. Applying TDA slightly decreases the BSE error irrespective of the starting eigenstates (the only exception being M06-HF/*aug*-cc-pVTZ). In other words, TDA

DOI: 10.1021/acs.jctc.6b01169
J. Chem. Theory Comput. 2017, 13, 767−783

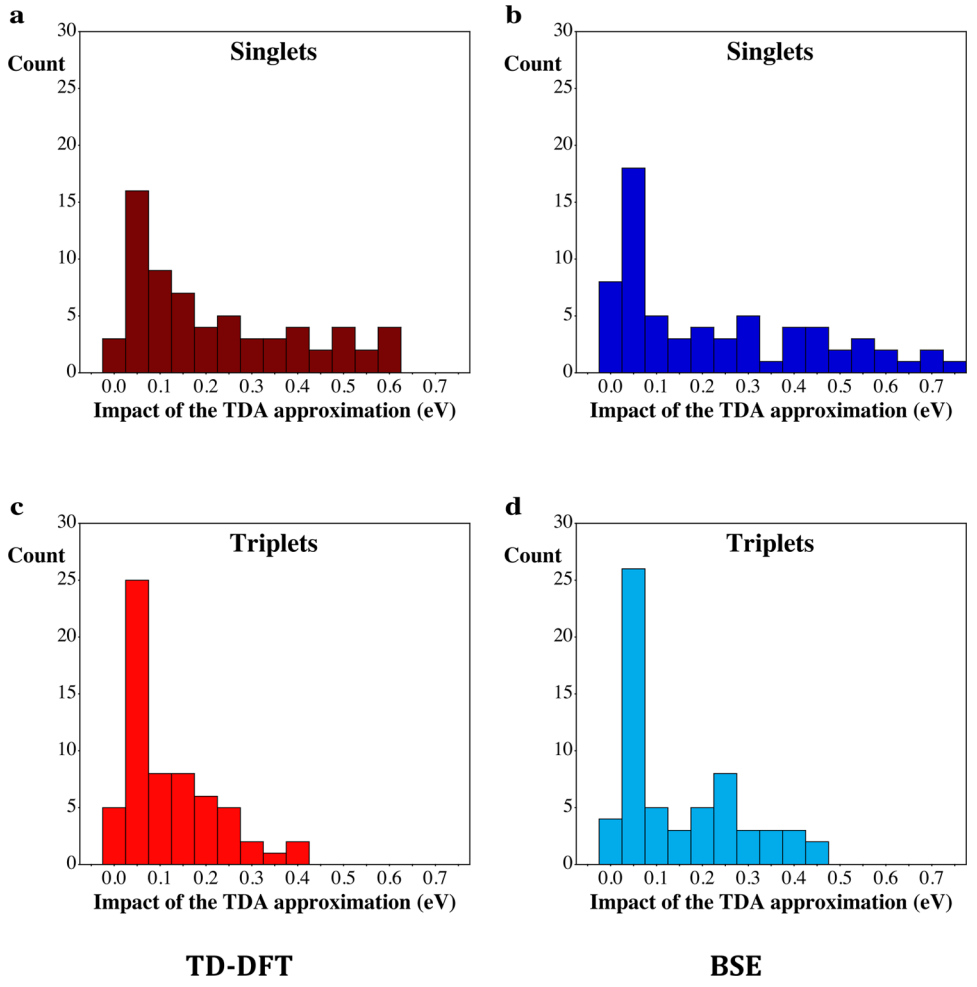

Figure 5. Histograms of the impact of the TDA approximation on the $\Delta E_{S0}S_n$ (top, a and b) and $\Delta E_{S0}T_n$ (bottom, c and d) transition energies determined with TD-DFT (left) and BSE/ev*GW* (right). All results are obtained using the M06-2X/TZVP approach.

does improve the BSE/ev*GW* estimates of the $\Delta E_{S_0T_n}$ transition (e.g., compare Figures 3c and d). Nevertheless, both TD-M06-2X and TDA-M06-2X outperform the corresponding BSE/ev*GW* methods for the S_0 to T_1 transitions (see Figures 3a and b) and therefore remain very valuable approaches in terms of the cost/quality balance. As seen in Table 2, this TD-DFT success is related to the selection of M06-2X, one of the best performing XCF for this property. Indeed, the TD-DFT M06-L, M06, and M06-HF errors are larger, and, for the same set of states, most other XCF provide much larger deviations, e.g., CAM-B3LYP (B98) delivers a MSE of −0.41 (−0.37) eV and a MAE of 0.42 (0.37) eV with TZVP.[9] We also highlight that TDA-M06-2X and TD-M06-2X statistical data are very similar for both tested basis sets but for the MSE that is smaller with the former approach. These conclusions are in line with the analysis of Peach and Tozer who found that the improvements brought by TDA are smaller than the one obtained by choosing an "adequate" XCF.[12]

3.4. Impact of the Tamm-Dancoff Approximation. As we have seen above, applying the TDA increases the computed transition energies, but this effect is significantly dependent on the considered molecule, on the spin-symmetry, and on the chemical nature of the considered state. To provide a more general overview of the impact of TDA, we report in Figure 5 histograms obtained by considering all M06-2X/TZVP transitions of Table 1. The corresponding *aug*-cc-pVTZ representation can be found in Figure S7 of the SI. Irrespective of the considered case (singlets versus triplets, TD-DFT versus BSE), one notices TDA induces an increase in the 0.00−0.20 eV range in most cases, though much larger variations are noticed for a few transitions. In Figure 5, besides the fact that a larger spread is found for singlet than triplet ES, there is no crystal-clear relationship between the amplitude of the impact of TDA and the nature of the ES, nor the selected theoretical models. Indeed, the mean variations of the transition energy induced by TDA for the BSE/ev*GW*@M06-2X data (0.23 eV for singlets and 0.15 eV for triplets) are only very slightly exceeding their TD-M06-2X counterparts (0.22 eV for singlets and 0.11 eV for triplets). Similar trends are obtained with the larger basis set with variations of 0.21 eV (0.17 eV) and 0.15 eV (0.13 eV) for respectively the singlet and triplet ES using BSE (TD-DFT). Overall, these trends are consistent with a recent BSE investigation of the lowest singlet and triplet ES of sexithiophene, where it was found that TDA induces upshifts of the transition energy by ca. 0.10−0.20 eV for these two states.[77] The same group also obtained similar conclusions for pentacene.[78] There is also a high degree of correlation between the upshifts induced by TDA on the TD-DFT and BSE transition energies, at least at the M06-2X/TZVP level. Indeed, we found correlation coefficients of 0.95 (singlet) and 0.90 (triplet) between these variations (see Figure S8 in the SI). In contrast, we found no correlation between the magnitude of the

DOI: 10.1021/acs.jctc.6b01169
J. Chem. Theory Comput. 2017, 13, 767−783

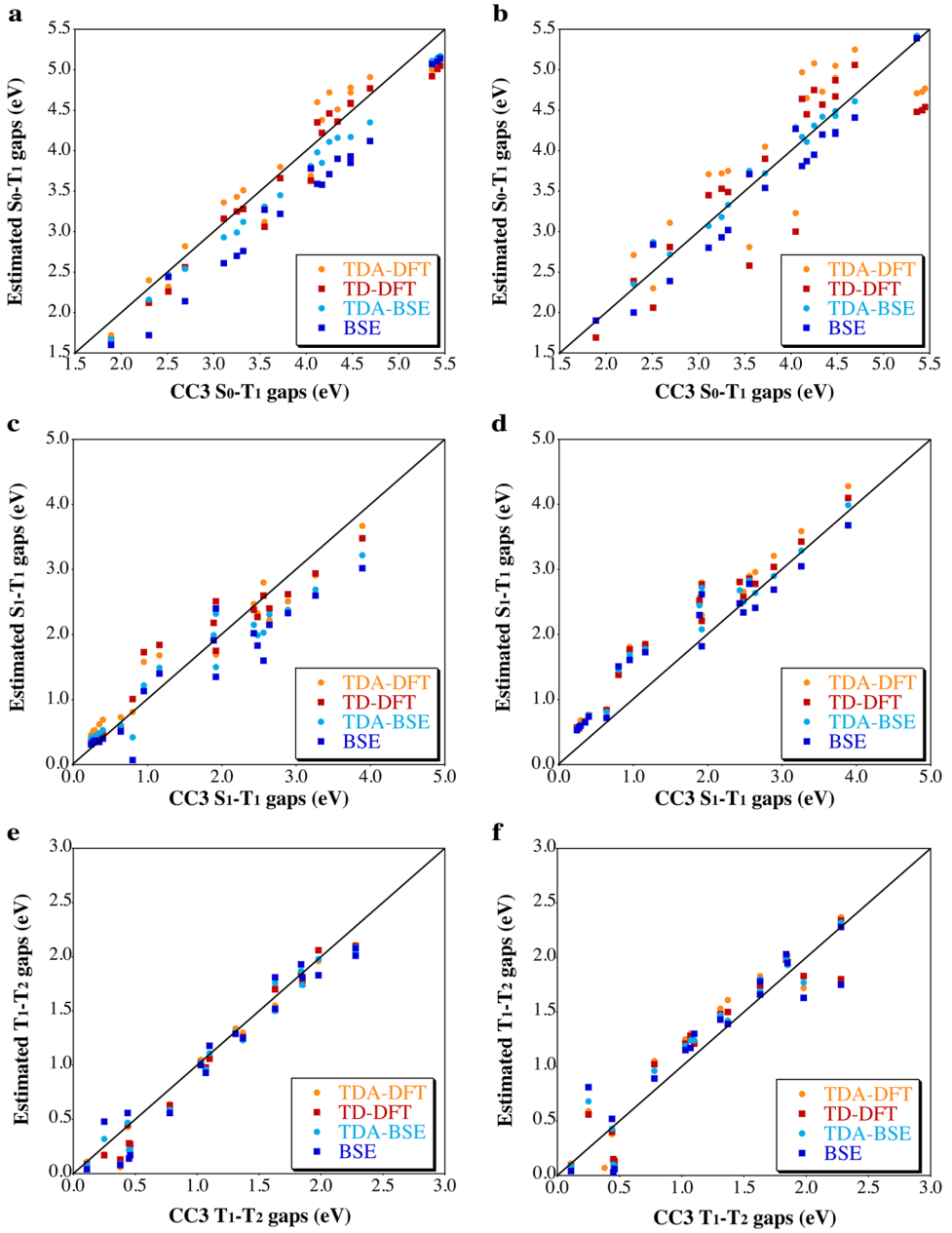

Figure 6. Comparisons between the TD-DFT and BSE description of $\Delta E_{S_0T_1}$ (top, a and b), $\Delta E_{S_1T_1}$ (center, c and d), and $\Delta E_{T_1T_2}$ (bottom, e and f) energy gaps for all considered molecules. The data obtained with M06-2X (M06-HF) are shown on the left-hand side (right-hand side). All values are in eV, use CC3 data as references, and rely on the TZVP basis set. The corresponding *aug*-cc-pVTZ results can be found in Figure S9 in the SI.

TDA correction for the triplet ES and the error of BSE nor TD-DFT (see Figure S9 in the SI). In short, though the obtained shifts are obviously strongly molecule dependent, the effects of TDA are, on average, similar for the two families of states and for the two theoretical approaches.

3.5. ES Splittings. As stated in the Introduction, it is important for many practical applications to obtain accurate energy splittings between the different states, besides the transition energies from the GS. In Figure 6 we compare the S_0-T_1, S_1-T_1, and T_1-T_2 gaps, determined for eight selected levels of theory to reference CC3 values. A statistical analysis is given in Table 3 for these three splittings. Section S7 in the SI provides the same information for all other approaches. A first noticeable point is that large high correlations with the reference values ($R > 0.96$) are systematically obtained with M06-2X/TZVP. This is true also for the M06-2X/*aug*-cc-pVTZ results but for one exception (full BSE for $\Delta E_{T_1}T_2$, see Table S16). For the $\Delta E_{S_0}T_1$, the computed average deviations are in line with those noted in Table 2, indicating that the lowest singlet−triplet transition is not more nor less accurately described than the transitions to the higher lying triplet ES. This conclusion is in line with previous works,[58,65] arguing that BSE/ev*GW* tends to perform similarly for both low-lying valence ES and higher-lying ES. As can be seen in Figure 6a, BSE/ev*GW*@M06-2X energies are too small and the application of TDA only slightly decreases this larger error, whereas (TDA-)BSE/ev*GW*@M06-HF $\Delta E_{S_0}T_1$ are significantly more accurate (Figure 6b), and this approach even outperforms TD-M06-2X if the TZVP atomic basis set is selected (see Table 3).

DOI: 10.1021/acs.jctc.6b01169
J. Chem. Theory Comput. 2017, 13, 767−783

Table 3. Statistical Analysis of the Errors Provided by TDA-DFT, TD-DFT, TDA-BSE/ev*GW*, and BSE/ev*GW* for Several Typical Splitting Energies Determined with TZVP[a]

		$\Delta E_{S_0T_1}$					
method	XCF	MSE	MAE	RMS	Max(+)	Max(−)	*R*
TDA-DFT	M06-2X	0.04	0.26	0.28	0.48	−0.43	0.96
	M06-HF	0.15	0.53	0.57	0.85	−0.82	0.85
TD-DFT	M06-2X	−0.11	0.20	0.25	0.23	−0.49	0.98
	M06-HF	−0.09	0.45	0.55	0.52	−1.05	0.86
TDA-BSE	M06-2X	−0.22	0.22	0.24		−0.34	1.00
	M06-HF	0.06	0.09	0.13	0.36	−0.08	0.99
BSE	M06-2X	−0.45	0.45	0.47		−0.63	0.99
	M06-HF	−0.12	0.23	0.25	0.32	−0.33	0.98
		$\Delta E_{S_1T_1}$					
method	XCF	MSE	MAE	RMS	Max(+)	Max(−)	*R*
TDA-DFT	M06-2X	0.42	0.43	0.46	0.88		0.99
	M06-HF	0.43	0.43	0.47	0.88		0.98
TD-DFT	M06-2X	0.36	0.36	0.39	0.67		0.99
	M06-HF	0.37	0.37	0.43	0.85		0.98
TDA-BSE	M06-2X	0.31	0.31	0.35	0.64		0.99
	M06-HF	0.32	0.32	0.40	0.80		0.98
BSE	M06-2X	0.21	0.24	0.29	0.57	−0.19	0.99
	M06-HF	0.21	0.32	0.37	0.71	−0.23	0.97
		$\Delta E_{T_1T_2}$					
method	XCF	MSE	MAE	RMS	Max(+)	Max(−)	*R*
TDA-DFT	M06-2X	−0.09	0.10	0.14	0.10	−0.32	0.99
	M06-HF	0.02	0.23	0.26	0.34	−0.52	0.94
TD-DFT	M06-2X	−0.08	0.10	0.12	0.08	−0.25	0.99
	M06-HF	0.01	0.19	0.23	0.31	−0.48	0.95
TDA-BSE	M06-2X	−0.09	0.11	0.15	0.13	−0.29	0.99
	M06-HF	−0.01	0.20	0.24	0.43	−0.53	0.94
BSE	M06-2X	−0.08	0.16	0.18	0.23	−0.31	0.97
	M06-HF	−0.02	0.21	0.27	0.56	−0.53	0.93

[a]The CC3 values of Table 1 are used as reference, and the CC3 method is used to determine the lowest states of the different spin symmetries. When reversal of two states appears with other approaches, the absolute value is used in the comparisons.

The situation significantly differs for the $\Delta E_{S1}T_1$ splittings that are essential for TADF. In this case, the BSE/ev*GW*@M06-2X and BSE/ev*GW*@M06-HF values are on average too large with the two atomic basis sets, whereas the corresponding TD-DFT values are too large with TZVP (Figures 6c and d) and too small with *aug*-cc-pVTZ (Figure S11). This result is due to the fact that BSE/*GW* presents a sensitivity to basis set effects comparable to the one of highly correlated wave function approaches (and hence they evolve similarly),[60] whereas TD-DFT values are significantly less basis set sensitive. The sign of the BSE $\Delta E_{S1}T_1$ errors is consistent with the seminal work of Louie, Cohen, and co-workers who reported a BSE splitting of 0.7 eV in silane, ca. twice the reference value of 0.4 eV.[75] We note that for the $\Delta E_{S1}T_1$ splittings, the smallest TD-DFT errors are obtained with M06-L (MAE of 0.20 eV, see Table S15), and the smallest BSE errors are reached with M06-2X (MAE of 0.24 eV, see Table 3), the latter approach providing a very large correlation with the reference values (middle left panel of Figure 6).

Finally, as illustrated in Figures 6e and f and S11, most of the tested theoretical models provide rather accurate triplet−triplet energy gaps with typical MAE in the 0.10−0.20 eV range, BSE/ev*GW*@M06-L yielding the poorest estimates (MAE of 0.33 eV). Using TDA allows reducing the BSE average absolute deviation to 0.11 or 0.12 eV when using M06-2X and the TZVP or *aug*-cc-pVTZ atomic basis sets, respectively, an accuracy comparable to the one attained with TDA-DFT and TD-DFT (0.10 and 0.14 eV, respectively). It is not a surprise that the splittings between ES of the same spin symmetry are easier to determine than those in which the spin symmetry is modified, as the latter involve larger differential correlation effects.

4. CONCLUSIONS

We have determined more than 60 singlet and 60 triplet transition energies on Thiel's molecular set using a Bethe-Salpeter method based on *GW* quasiparticle energies that were self-consistently converged with respect to the starting DFT eigenvalues. Two atomic basis sets were used. By using the four members of the M06 family to generate the starting eigenstates, we evaluated the impact of the partially self-consistent *GW* procedure. For the singlet excited-states, the effect is impressive: the ev*GW* approach allows washing out the majority of the XCF dependency, and except when M06-HF − a XCF with 100% of *exact* exchange − is used, all statistical parameters are similar for the members of the M06 family. In addition, consistently with our previous works,[58,59] the obtained singlet ES were found to be rather accurate. For the triplet excited-states, ev*GW* also greatly reduces the impact of the selected XCF compared to the perturbative G_0W_0 scheme, but the improvements are less spectacular than for the singlet ES, hinting that the form of the eigenfunctions has more influence for the former ES. Paralleling previously obtained BSE/G_0W_0 values,[57] we found that the triplet ES are significantly overstabilized by BSE/ev*GW*, though the dramatic underestimation of triplet energies obtained with BSE/G_0W_0 calculations based on XCF with none or a small amount of exact exchange is significantly corrected. In fact, the only BSE variant yielding a positive average deviation is BSE/ev*GW*@M06-HF/*aug*-cc-pVTZ. This is however due to the presence of intruder eigenstates that yield state mixing. As a consequence, this approach delivers poorer correlations with respect to the reference values than all the other tested BSE approaches, and one cannot recommend such a method. Our results indicate that, at this stage, using TD-DFT with a well-chosen XCF is probably a more effective option than BSE/ev*GW* to estimate $\Delta E_{S0}T_1$. Indeed, while the smallest MAE was reached with TDA-BSE/ev*GW*@M06-HF/TZVP (0.17 eV, Table 2), TD-M06-2X yields only slightly larger errors (MAE of 0.22 eV) but is much less sensitive to the selected atomic basis set. Moreover, we found that the application of the Tamm-Dancoff approximation tends to increase the GS to ES transition energies by an average of ca. 0.20 eV and that the magnitude of this effect is slightly larger for singlet than triplet ES but similar

DOI: 10.1021/acs.jctc.6b01169
J. Chem. Theory Comput. 2017, 13, 767−783

for TD-DFT and BSE. By considering the full set of molecules, we noticed that TDA helps improving the (generally too small) BSE/ev*GW* estimates. The question whether TDA improves the triplets (blueshift) for the same reasons that it destabilizes the singlets or by a mechanism related to the reduction of triplet state instability as proposed at the TD-DFT level[10,11,98] remains to be determined. The errors obtained with BSE for the S_1-T_1 splittings are globally of the same order of magnitude as their TD-DFT counterparts (ca. 0.20−0.40 eV), though the best performing XCF differ (M06-L with TD-DFT, M06-2X with BSE). Whether this finding is valid only for the small- and medium-sized compounds treated here or also pertains for the large charge-transfer dyes of practical interest for TADF applicationscannot be answered with the present set of data. In contrast the triplet−triplet energy gaps are accurately estimated by all approaches, e.g., TDA-BSE/ev*GW*@M06-2X leads to a mean absolute error of 0.11 eV, equivalent to the 0.10 eV error obtained with TDA-M06-2X.

The understanding of the origin of the significant BSE underestimations goes certainly beyond this study. The so-called triplet instability problem, documented within TD-HF and TDDFT for more than five years,[10−12] still remains an issue of discussion: while a proper diagnostic of triplet underestimation has been proposed by comparing the TDDFT equation to the DFT stability equations, a proper cure of the problem remains to be found. It can be emphasized along that line that the BSE formalism suffers from the impossibility to "tune" the functional: in the calculations presented above, variations in the BSE triplet excitation energies originate mainly from changing the Kohn−Sham initial eigenstates, while the functional form of the BSE equations remains unchanged. In this general framework of comparison between BSE and TD-DFT approaches, determining BSE singlet−triplet transition energies on the basis of fully self-consistent *GW* quasiparticle energies would also be useful, as the dependency from the starting KS eigenstates would disappear.

In short, this first work comes as an important warning − BSE/*GW* might be well suited for singlet ES but not for triplet ES − and might also constitute the start of the search for the understanding of the fundamental reasons of this problem.

■ ASSOCIATED CONTENT

Supporting Information

The Supporting Information is available free of charge on the ACS Publications website at DOI: 10.1021/acs.jctc.6b01169.

Numerical data for the five test compounds of Figures 1 and 2 and corresponding *aug*-cc-pVTZ values; TDA-DFT, TD-DFT, BSE, and TDA-BSE results with M06-L (TZVP), M06 (TZVP), M06-2X (*aug*-cc-pVTZ), and M06-HF (*aug*-cc-pVTZ) XCF; extra comparison plots obtained M06-L (TZVP), M06 (TZVP), M06-2X (*aug*-cc-pVTZ), and M06-HF (*aug*-cc-pVTZ) XCF; additional statistical data for the full set; impact of TDA: large basis set and correlation; additional splittings figures and statistics (PDF)

■ AUTHOR INFORMATION

Corresponding Authors

*E-mail: Denis.Jacquemin@univ-nantes.fr.
*E-mail: xavier.blase@neel.cnrs.fr.

ORCID

Denis Jacquemin: 0000-0002-4217-0708

Ivan Duchemin: 0000-0003-4713-1174

Notes

The authors declare no competing financial interest.

■ ACKNOWLEDGMENTS

D.J. is indebted to Dr. D. Escudero for enlightening discussions about TADF and SF dyes. D.J. acknowledges the European Research Council (ERC) and the *Région des Pays de la Loire* for financial support in the framework of a Starting Grant (Marches -278845) and the LumoMat project, respectively. This research used resources of (i) the GENCI-CINES/IDRIS; (ii) CCIPL (*Centre de Calcul Intensif des Pays de Loire*); (iii) a local Troy cluster, and (iv) HPC resources from ArronaxPlus (grant ANR-11-EQPX-0004 funded by the French National Agency for Research).

■ REFERENCES

(1) *Organic Optoelectronic Materials*; Li, Y., Ed.; Lecture Notes in Chemistry; Springer, 2015; pp 1−392.
(2) Uoyama, H.; Goushi, K.; Shizu, K.; Nomura, H.; Adachi, C. Highly Efficient Organic Light-Emitting Diodes from Delayed Fluorescence. *Nature* **2012**, *492*, 234−238.
(3) Singh-Rachford, T. N.; Castellano, F. N. Photon Upconversion Based on Sensitized Triplet-Triplet Annihilation. *Coord. Chem. Rev.* **2010**, *254*, 2560−2573.
(4) Zhao, J.; Ji, S.; Guo, H. Triplet-Triplet Annihilation Based Upconversion: From Triplet Sensitizers and Triplet Acceptors to Upconversion Quantum Yields. *RSC Adv.* **2011**, *1*, 937−950.
(5) Tao, Y.; Yuan, K.; Chen, T.; Xu, P.; Li, H.; Chen, R.; Zheng, C.; Zhang, L.; Huang, W. Thermally Activated Delayed Fluorescence Materials Towards the Breakthrough of Organoelectronics. *Adv. Mater.* **2014**, *26*, 7931−7958.
(6) Congreve, D. N.; Lee, J.; Thompson, N. J.; Hontz, E.; Yost, S. R.; Reusswig, P. D.; Bahlke, M. E.; Reineke, S.; Van Voorhis, T.; Baldo, M. A. External Quantum Efficiency Above 100% in a Singlet-Exciton-Fission-Based Organic Photovoltaic Cell. *Science* **2013**, *340*, 334−337.
(7) Chou, P.-Y.; Chou, H.-H.; Chen, Y.-H.; Su, T.-H.; Liao, C.-Y.; Lin, H.-W.; Lin, W.-C.; Yen, H.-Y.; Chen, I.-C.; Cheng, C.-H. Efficient Delayed Fluorescence via Triplet-Triplet Annihilation for Deep-Blue Electroluminescence. *Chem. Commun.* **2014**, *50*, 6869−6871.
(8) Sancho-García, J. C. Treatment of Singlet-Triplet Splitting of a Set of Phenylene Ethylenes Organic Molecules by TD-DFT. *Chem. Phys. Lett.* **2007**, *439*, 236−242.
(9) Jacquemin, D.; Perpète, E. A.; Ciofini, I.; Adamo, C. Assessment of Functionals for TD-DFT Calculations of Singlet-Triplet Transitions. *J. Chem. Theory Comput.* **2010**, *6*, 1532−1537.
(10) Peach, M. J. G.; Williamson, M. J.; Tozer, D. J. Influence of Triplet Instabilities in TDDFT. *J. Chem. Theory Comput.* **2011**, *7*, 3578−3585.
(11) Sears, J. S.; Koerzdoerfer, T.; Zhang, C. R.; Brédas, J. L. Orbital Instabilities and Triplet States From Time-Dependent Density Functional Theory and Long-Range Corrected Functionals. *J. Chem. Phys.* **2011**, *135*, 151103.
(12) Peach, M. J. G.; Tozer, D. J. Overcoming Low Orbital Overlap and Triplet Instability Problems in TDDFT. *J. Phys. Chem. A* **2012**, *116*, 9783−9789.
(13) Bousquet, D.; Fukuda, R.; Jacquemin, D.; Ciofini, I.; Adamo, C.; Ehara, M. Benchmark Study on the Triplet Excited-State Geometries and Phosphorescence Energies of Heterocyclic Compounds: Comparison Between TD-PBE0 and SAC-CI. *J. Chem. Theory Comput.* **2014**, *10*, 3969−3979.
(14) Niehaus, T. A.; Hofbeck, T.; Yersin, H. Charge-Transfer Excited States in Phosphorescent Organo-Transition Metal Compounds: A Difficult Case for Time Dependent Density Functional Theory? *RSC Adv.* **2015**, *5*, 63318−63329.

DOI: 10.1021/acs.jctc.6b01169
J. Chem. Theory Comput. 2017, 13, 767−783

(15) Jacquemin, D.; Adamo, C. In *Density-Functional Methods for Excited States*; Ferré, N., Filatov, M., Huix-Rotllant, M. Springer International Publishing: Cham, 2016; Vol. *368*, pp 347−375.
(16) Sun, H.; Zhong, C.; Brédas, J.-L. Reliable Prediction with Tuned Range-Separated Functionals of the Singlet-Triplet Gap in Organic Emitters for Thermally Activated Delayed Fluorescence. *J. Chem. Theory Comput.* **2015**, *11*, 3851−3858.
(17) Brückner, C.; Engels, B. Benchmarking Singlet and Triplet Excitation Energies of Molecular Semiconductors for Singlet Fission: Tuning the Amount of HF Exchange and Adjusting Local Correlation to Obtain Accurate Functionals for Singlet-Triplet Gaps. *Chem. Phys.* **2016**, DOI: 10.1016/j.chemphys.2016.08.023.
(18) Baer, R.; Livshits, E.; Salzner, U. Tuned Range-Separated Hybrids in Density Functional Theory. *Annu. Rev. Phys. Chem.* **2010**, *61*, 85−109.
(19) Christiansen, O.; Koch, H.; Jørgensen, P. The Second-Order Approximate Coupled Cluster Singles and Doubles Model CC2. *Chem. Phys. Lett.* **1995**, *243*, 409−418.
(20) Zhekova, H.; Krykunov, M.; Autschbach, J.; Ziegler, T. Applications of Time Dependent and Time Independent Density Functional Theory to the First π to $\pi^{\star}$ Transition in Cyanine Dyes. *J. Chem. Theory Comput.* **2014**, *10*, 3299−3307.
(21) Andrzejak, M.; Szczepanik, D. W.; Orzel, L. The Lowest Triplet States of Bridged Cis-2,2[Prime or Minute]-Bithiophenes - Theory vs. Experiment. *Phys. Chem. Chem. Phys.* **2015**, *17*, 5328−5337.
(22) Momeni, M. R.; Brown, A. A Local CC2 and TDA-DFT Double Hybrid Study on BODIPY/aza-BODIPY Dimers as Heavy Atom Free Triplet Photosensitizers for Pho- todynamic Therapy Applications. *J. Phys. Chem. A* **2016**, *120*, 2550−2560.
(23) Alary, F.; Heully, J.-L.; Bijeire, L.; Vicendo, P. Is the 3MLCT the Only Photoreactive State of Polypyridyl Complexes? *Inorg. Chem.* **2007**, *46*, 3154−3165.
(24) González, L.; Escudero, D.; Serrano-Andrès, L. Progress and Challenges in the Calculation of Electronic Excited States. *ChemPhysChem* **2012**, *13*, 28−51.
(25) Moore, B., II; Autschbach, J. Longest-Wavelength Electronic Excitations of Linear Cyanines: The Role of Electron Delocalization and of Approximations in Time-Dependent Density Functional Theory. *J. Chem. Theory Comput.* **2013**, *9*, 4991−5003.
(26) Hait, D.; Zhu, T.; McMahon, D. P.; Van Voorhis, T. Prediction of Excited-State Energies and Singlet-Triplet Gaps of Charge-Transfer States Using a Restricted Open-Shell Kohn-Sham Approach. *J. Chem. Theory Comput.* **2016**, *12*, 3353−3359.
(27) Sham, L. J.; Rice, T. M. Many-Particle Derivation of the Effective-Mass Equation for the Wannier Exciton. *Phys. Rev.* **1966**, *144*, 708−714.
(28) Hanke, W.; Sham, L. J. Many-Particle Effects in the Optical Excitations of a Semiconductor. *Phys. Rev. Lett.* **1979**, *43*, 387−390.
(29) Strinati, G. Dynamical Shift and Broadening of Core Excitons in Semiconductors. *Phys. Rev. Lett.* **1982**, *49*, 1519−1522.
(30) Onida, G.; Reining, L.; Rubio, A. Electronic Excitations: Density-Functional Versus Many-Body Green's-Function Approaches. *Rev. Mod. Phys.* **2002**, *74*, 601−659.
(31) Tiago, M. L.; Chelikowsky, J. R. First-Principles GW-BSE Excitations in Organic Molecules. *Solid State Commun.* **2005**, *136*, 333−337.
(32) Tiago, M. L.; Kent, P. R. C.; Hood, R. Q.; Reboredo, F. A. Neutral and Charged Excitations in Carbon Fullerenes From First-Principles Many-Body Theories. *J. Chem. Phys.* **2008**, *129*, 084311.
(33) Ma, Y.; Rohlfing, M.; Molteni, C. Excited States of Biological Chromophores Studied Using Many-Body Perturbation Theory: Effects of Resonant-Antiresonant Coupling and Dynamical Screening. *Phys. Rev. B: Condens. Matter Mater. Phys.* **2009**, *80*, 241405.
(34) Palummo, M.; Hogan, C.; Sottile, F.; Bagalá, P.; Rubio, A. Ab Initio Electronic and Optical Spectra of Free-Base Porphyrins: The Role of Electronic Correlation. *J. Chem. Phys.* **2009**, *131*, 084102.
(35) Kaczmarski, M. S.; Ma, Y.; Rohlfing, M. Diabatic States of a Photoexcited Retinal Chromophore From *Ab Initio* Many-Body Perturbation Theory. *Phys. Rev. B: Condens. Matter Mater. Phys.* **2010**, *81*, 115433.
(36) Ma, Y.; Rohlfing, M.; Molteni, C. Modeling the Excited States of Biological Chromophores within Many-Body Green's Function Theory. *J. Chem. Theory Comput.* **2010**, *6*, 257−265.
(37) Rocca, D.; Lu, D.; Galli, G. Ab Initio Calculations of Optical Absorption Spectra: Solution of the Bethe-Salpeter Equation Within Density Matrix Perturbation Theory. *J. Chem. Phys.* **2010**, *133*, 164109.
(38) Garcia-Lastra, J. M.; Thygesen, K. S. Renormalization of Optical Excitations in Molecules near a Metal Surface. *Phys. Rev. Lett.* **2011**, *106*, 187402.
(39) Blase, X.; Attaccalite, C. Charge-Transfer Excitations in Molecular Donor-Acceptor Complexes Within the Many-Body Bethe-Salpeter Approach. *Appl. Phys. Lett.* **2011**, *99*, 171909.
(40) Duchemin, I.; Deutsch, T.; Blase, X. Short-Range to Long-Range Charge-Transfer Excitations in the Zincbacteriochlorin-Bacteriochlorin Complex: A Bethe-Salpeter Study. *Phys. Rev. Lett.* **2012**, *109*, 167801.
(41) Baumeier, B.; Andrienko, D.; Ma, Y.; Rohlfing, M. Excited States of Dicyanovinyl-Substituted Oligothiophenes from Many-Body Green's Functions Theory. *J. Chem. Theory Comput.* **2012**, *8*, 997−1002.
(42) Faber, C.; Duchemin, I.; Deutsch, T.; Blase, X. Many-Body Green's Function Study of Coumarins for Dye-Sensitized Solar Cells. *Phys. Rev. B: Condens. Matter Mater. Phys.* **2012**, *86*, 155315.
(43) Hogan, C.; Palummo, M.; Gierschner, J.; Rubio, A. Correlation Effects in the Optical Spectra of Porphyrin Oligomer Chains: Exciton Confinement and Length Dependence. *J. Chem. Phys.* **2013**, *138*, 024312.
(44) Faber, C.; Boulanger, P.; Duchemin, I.; Attaccalite, C.; Blase, X. Many-Body Greens Function GW and Bethe-Salpeter Study of the Optical Excitations in a Paradigmatic Model Dipeptide. *J. Chem. Phys.* **2013**, *139*, 194308.
(45) Duchemin, I.; Blase, X. Resonant Hot Charge-Transfer Excitations in Fullerene-Porphyrin Complexes: Many-Body Bethe-Salpeter Study. *Phys. Rev. B: Condens. Matter Mater. Phys.* **2013**, *87*, 245412.
(46) Varsano, D.; Coccia, E.; Pulci, O.; Mosca Conte, A.; Guidoni, L. Ground State Structures and Electronic Excitations of Biological Chromophores at Quantum Monte Carlo/Many Body Green's Function Theory Level. *Comput. Theor. Chem.* **2014**, *1040-1041*, 338−346.
(47) Coccia, E.; Varsano, D.; Guidoni, L. Ab Initio Geometry and Bright Excitation of Carotenoids: Quantum Monte Carlo and Many Body Greens Function Theory Calculations on Peridinin. *J. Chem. Theory Comput.* **2014**, *10*, 501−506.
(48) Baumeier, B.; Rohlfing, M.; Andrienko, D. Electronic Excitations in Push-Pull Oligomers and Their Complexes with Fullerene from Many-Body Green's Functions Theory with Polarizable Embedding. *J. Chem. Theory Comput.* **2014**, *10*, 3104−3110.
(49) Boulanger, P.; Jacquemin, D.; Duchemin, I.; Blase, X. Fast and Accurate Electronic Excitations in Cyanines with the Many-Body Bethe-Salpeter Approach. *J. Chem. Theory Comput.* **2014**, *10*, 1212−1218.
(50) Boulanger, P.; Chibani, S.; Le Guennic, B.; Duchemin, I.; Blase, X.; Jacquemin, D. Combining the Bethe-Salpeter Formalism with Time-Dependent DFT Excited-State Forces to Describe Optical Signatures: NBO Fluoroborates as Working Examples. *J. Chem. Theory Comput.* **2014**, *10*, 4548−4556.
(51) Koval, P.; Foerster, D.; Sánchez-Portal, D. Fully Self-Consistent *GW* and Quasiparticle Self-Consistent *GW* for Molecules. *Phys. Rev. B: Condens. Matter Mater. Phys.* **2014**, *89*, 155417.
(52) Körbel, S.; Boulanger, P.; Duchemin, I.; Blase, X.; Marques, M. A. L.; Botti, S. Benchmark Many-Body GW and BetheSalpeter Calculations for Small Transition Metal Molecules. *J. Chem. Theory Comput.* **2014**, *10*, 3934−3943.
(53) Hahn, T.; Geiger, J.; Blase, X.; Duchemin, I.; Niedzialek, D.; Tscheuschner, S.; Beljonne, D.; Bässler, H.; Köhler, A. Does Excess

Energy Assist Photogeneration in an Organic Low-Bandgap Solar Cell? *Adv. Funct. Mater.* **2015**, *25*, 1287−1295.
(54) Krause, K.; Harding, M. E.; Klopper, W. Coupled-Cluster Reference Values for the GW27 and GW100 Test Sets for the Assessment of GW Methods. *Mol. Phys.* **2015**, *113*, 1952−1960.
(55) Hirose, D.; Noguchi, Y.; Sugino, O. All-Electron *GW*+Bethe-Salpeter Calculations on Small Molecules. *Phys. Rev. B: Condens. Matter Mater. Phys.* **2015**, *91*, 205111.
(56) Ljungberg, M. P.; Koval, P.; Ferrari, F.; Foerster, D.; Sanchez-Portal, D. Cubic-Scaling Iterative Solution of the Bethe-Salpeter Equation for Finite Systems. *Phys. Rev. B: Condens. Matter Mater. Phys.* **2015**, *92*, 075422.
(57) Bruneval, F.; Hamed, S. M.; Neaton, J. B. A Systematic Benchmark of the Ab Initio Bethe-Salpeter Equation Approach for Low-Lying Optical Excitations of Small Organic Molecules. *J. Chem. Phys.* **2015**, *142*, 244101.
(58) Jacquemin, D.; Duchemin, I.; Blase, X. Benchmarking the Bethe-Salpeter Formalism on a Standard Organic Molecular Set. *J. Chem. Theory Comput.* **2015**, *11*, 3290−3304.
(59) Jacquemin, D.; Duchemin, I.; Blase, X. 0−0 Energies Using Hybrid Schemes: Benchmarks of TD-DFT, CIS(D), ADC(2), CC2 and BSE/GW formalisms for 80 Real-Life Compounds. *J. Chem. Theory Comput.* **2015**, *11*, 5340−5359.
(60) Jacquemin, D.; Duchemin, I.; Blase, X. Assessment of the Convergence of Partially Self-Consistent BSE/GW Calculations. *Mol. Phys.* **2016**, *114*, 957−967.
(61) Blase, X.; Boulanger, P.; Bruneval, F.; Fernandez-Serra, M.; Duchemin, I. GW and Bethe-Salpeter Study of Small Water Clusters. *J. Chem. Phys.* **2016**, *144*, 034109.
(62) Rebolini, E.; Toulouse, J. Range-Separated Time-Dependent Density-Functional Theory With a Frequency-Dependent Second-Order Bethe-Salpeter Correlation Kernel. *J. Chem. Phys.* **2016**, *144*, 094107.
(63) Jacquemin, D.; Duchemin, I.; Blondel, A.; Blase, X. Assessment of the Accuracy of the Bethe-Salpeter (BSE/GW) Oscillator Strengths. *J. Chem. Theory Comput.* **2016**, *12*, 3969−3981.
(64) Ziaei, V.; Bredow, T. GW-BSE Approach on S1 Vertical Transition Energy of Large Charge Transfer Compounds: A Performance Assessment. *J. Chem. Phys.* **2016**, *145*, 174305.
(65) Hung, L.; da Jornada, F. H.; Souto-Casares, J.; Chelikowsky, J. R.; Louie, S. G.; Öğüt, S. Excitation Spectra of Aromatic Molecules Within a Real-Space GW-BSE Formalism: Role of Self-Consistency and Vertex Corrections. *Phys. Rev. B: Condens. Matter Mater. Phys.* **2016**, *94*, 085125.
(66) Krause, K.; Klopper, W. Implementation of the Bethe-Salpeter Equation in the TURBOMOLE Program. *J. Comput. Chem.* **2017**, *38*, 383−388.
(67) Azarias, C.; Duchemin, I.; Blase, X.; Jacquemin, D. Bethe-Salpeter Study of Cationic Dyes: Comparisons with ADC(2) and TD-DFT. *J. Chem. Phys.* **2017**, *146*, 034301.
(68) Hedin, L. New Method for Calculating the One-Particle Green's Function with Application to the Electron-Gas Problem. *Phys. Rev.* **1965**, *139*, A796−A823.
(69) Hybertsen, M. S.; Louie, S. G. Electron Correlation in Semiconductors and Insulators: Band Gaps and Quasiparticle Energies. *Phys. Rev. B: Condens. Matter Mater. Phys.* **1986**, *34*, 5390−5413.
(70) Godby, R. W.; Schlüter, M.; Sham, L. J. Self-Energy Operators and Exchange-Correlation Potentials in Semiconductors. *Phys. Rev. B: Condens. Matter Mater. Phys.* **1988**, *37*, 10159−10175.
(71) van der Horst, J.-W.; Bobbert, P. A.; Michels, M. A. J.; Bässler, H. Calculation of Excitonic Properties of Conjugated Polymers Using the Bethe-Salpeter Equation. *J. Chem. Phys.* **2001**, *114*, 6950−6957.
(72) Konabe, S.; Watanabe, K. Mechanism for Optical Activation of Dark Spin-Triplet Excitons in Hydrogenated Single-Walled Carbon Nanotubes. *Phys. Rev. B: Condens. Matter Mater. Phys.* **2011**, *83*, 045407.
(73) Wang, S.; Wang, J. Quasiparticle Energies and Optical Excitations in Chevron-Type Graphene Nanoribbon. *J. Phys. Chem. C* **2012**, *116*, 10193−10197.
(74) Li, L.-H.; Kontsevoi, O. Y.; Freeman, A. J. Electronic and Optical Excitations of the PTB7 Crystal: First-Principles GW-BSE Calculations. *Phys. Rev. B: Condens. Matter Mater. Phys.* **2014**, *90*, 195203.
(75) Grossman, J. C.; Rohlfing, M.; Mitas, L.; Louie, S. G.; Cohen, M. L. High Accuracy Many-Body Calculational Approaches for Excitations in Molecules. *Phys. Rev. Lett.* **2001**, *86*, 472−475.
(76) Despoja, V.; Lončarić, I.; Mowbray, D. J.; Marušić, L. Quasiparticle Spectra and Excitons of Organic Molecules Deposited on Substrates: G_0W_0-BSE Approach Applied to Benzene on Graphene and Metallic Substrates. *Phys. Rev. B: Condens. Matter Mater. Phys.* **2013**, *88*, 235437.
(77) Leng, X.; Yin, H.; Liang, D.; Ma, Y. Excitons and Davydov Splitting in Sexithiophene From First-Principles Many-Body Green's Function Theory. *J. Chem. Phys.* **2015**, *143*, 114501.
(78) Leng, X.; Feng, J.; Chen, T.; Liu, C.; Ma, Y. Optical Properties of Acene Molecules and Pentacene Crystal From the Many-Body Green'S Function Method. *Phys. Chem. Chem. Phys.* **2016**, *18*, 30777−30784.
(79) Schreiber, M.; Silva-Junior, M. R.; Sauer, S. P. A.; Thiel, W. Benchmarks for Electronically Excited States: CASPT2, CC2, CCSD and CC3. *J. Chem. Phys.* **2008**, *128*, 134110.
(80) Sauer, S. P. A.; Schreiber, M.; Silva-Junior, M. R.; Thiel, W. Benchmarks for Electronically Excited States: A Comparison of Noniterative and Iterative Triples Corrections in Linear Response Coupled Cluster Methods: CCSDR(3) versus CC3. *J. Chem. Theory Comput.* **2009**, *5*, 555−564.
(81) Silva-Junior, M. R.; Sauer, S. P. A.; Schreiber, M.; Thiel, W. Basis Set Effects on Coupled Cluster Benchmarks of Electronically Excited States: CC3, CCSDR(3) and CC2. *Mol. Phys.* **2010**, *108*, 453−465.
(82) Silva-Junior, M. R.; Schreiber, M.; Sauer, S. P. A.; Thiel, W. Benchmarks of Electronically Excited States: Basis Set Effecs Benchmarks of Electronically Excited States: Basis Set Effects on CASPT2 Results. *J. Chem. Phys.* **2010**, *133*, 174318.
(83) Sauer, S. P.; Pitzner-Frydendahl, H. F.; Buse, M.; Jensen, H. J. A.; Thiel, W. Performance of SOPPA-Based Methods in the Calculation of Vertical Excitation Energies and Oscillator Strengths. *Mol. Phys.* **2015**, *113*, 2026−2045.
(84) Blase, X.; Attaccalite, C.; Olevano, V. First-Principles *GW* Calculations for Fullerenes, Porphyrins, Phtalocyanine, and Other Molecules of Interest for Organic Photovoltaic Applications. *Phys. Rev. B: Condens. Matter Mater. Phys.* **2011**, *83*, 115103.
(85) Faber, C.; Attaccalite, C.; Olevano, V.; Runge, E.; Blase, X. First-Principles *GW* Calculations for DNA and RNA Nucleobases. *Phys. Rev. B: Condens. Matter Mater. Phys.* **2011**, *83*, 115123.
(86) Valiev, M.; Bylaska, E. J.; Govind, N.; Kowalski, K.; Straatsma, T. P.; Van Dam, H. J. J.; Wang, D.; Nieplocha, J.; Apra, E.; Windus, T. L.; de Jong, W. A. NWChem: a Comprehensive and Scalable Open-Source Solution for Large Scale Molecular Simulations. *Comput. Phys. Commun.* **2010**, *181*, 1477−1489.
(87) Zhao, Y.; Truhlar, D. G. The M06 Suite of Density Functionals for Main Group Thermochemistry, Thermochemical Kinetics, Noncovalent Interactions, Excited States, and Transition Elements: Two New Functionals and Systematic Testing of Four M06-Class Functionals and 12 Other Functionals. *Theor. Chem. Acc.* **2008**, *120*, 215−241.
(88) At the G_0W_0 level, slightly less KS levels were corrected with *GW* as only low-lying states have been considered. In all cases, all noncorrected KS energy levels are shifted rigidly in order to preserve the Kohn−Sham DFT spacing with the highest corrected virtual state.
(89) Weigend, F.; Köhn, A.; Hättig, C. Efficient Use of the Correlation Consistent Basis Sets in Resolution of the Identity MP2 Calculations. *J. Chem. Phys.* **2002**, *116*, 3175−3183.
(90) Frisch, M. J.; Trucks, G. W.; Schlegel, H. B.; Scuseria, G. E.; Robb, M. A.; Cheeseman, J. R.; Scalmani, G.; Barone, V.; Mennucci, B.; Petersson, G. A.; Nakatsuji, H.; Caricato, M.; Li, X.; Hratchian, H.

DOI: 10.1021/acs.jctc.6b01169
J. Chem. Theory Comput. 2017, 13, 767−783

P.; Izmaylov, A. F.; Bloino, J.; Zheng, G.; Sonnenberg, J. L.; Hada, M.; Ehara, M.; Toyota, K.; Fukuda, R.; Hasegawa, J.; Ishida, M.; Nakajima, T.; Honda, Y.; Kitao, O.; Nakai, H.; Vreven, T.; Montgomery, J. A., Jr.; Peralta, J. E.; Ogliaro, F.; Bearpark, M.; Heyd, J. J.; Brothers, E.; Kudin, K. N.; Staroverov, V. N.; Kobayashi, R.; Normand, J.; Raghavachari, K.; Rendell, A.; Burant, J. C.; Iyengar, S. S.; Tomasi, J.; Cossi, M.; Rega, N.; Millam, J. M.; Klene, M.; Knox, J. E.; Cross, J. B.; Bakken, V.; Adamo, C.; Jaramillo, J.; Gomperts, R.; Stratmann, R. E.; Yazyev, O.; Austin, A. J.; Cammi, R.; Pomelli, C.; Ochterski, J. W.; Martin, R. L.; Morokuma, K.; Zakrzewski, V. G.; Voth, G. A.; Salvador, P.; Dannenberg, J. J.; Dapprich, S.; Daniels, A. D.; Farkas, O.; Foresman, J. B.; Ortiz, J. V.; Cioslowski, J.; Fox, D. J. *Gaussian 09 Revision D.01*; Gaussian Inc.: Wallingford, CT, 2009.

(91) Silva-Junior, M. R.; Schreiber, M.; Sauer, S. P. A.; Thiel, W. Benchmarks for Electronically Excited States: Time-Dependent Density Functional Theory and Density Functional Theory Based Multireference Configuration Interaction. *J. Chem. Phys.* **2008**, *129*, 104103.

(92) Jacquemin, D.; Wathelet, V.; Perpète, E. A.; Adamo, C. Extensive TD-DFT Benchmark: Singlet-Excited States of Organic Molecules. *J. Chem. Theory Comput.* **2009**, *5*, 2420−2435.

(93) Grüning, M.; Marini, A.; Gonze, X. Exciton-Plasmon States in Nanoscale Materials: Breakdown of the Tamm-Dancoff Approximation. *Nano Lett.* **2009**, *9*, 2820−2824.

(94) Sander, T.; Maggio, E.; Kresse, G. Beyond the Tamm-Dancoff Approximation for Extended Systems Using Exact Diagonalization. *Phys. Rev. B: Condens. Matter Mater. Phys.* **2015**, *92*, 045209.

(95) Rangel, T.; Berland, K.; Sharifzadeh, S.; Brown-Altvater, F.; Lee, K.; Hyldgaard, P.; Kronik, L.; Neaton, J. B. Structural and Excited-State Properties of Oligoacene Crystals From First Principles. *Phys. Rev. B: Condens. Matter Mater. Phys.* **2016**, *93*, 115206.

(96) In that reference, other molecules for which TBE values were determined for the singlet states but not triplet states, e.g., the DNA bases, were included in the set, so that a perfectly balanced comparison is not possible

(97) Jacquemin, D.; Perpète, E. A.; Ciofini, I.; Adamo, C.; Valero, R.; Zhao, Y.; Truhlar, D. G. On the Performances of the M06 Family of Density Functionals for Electronic Excitation Energies. *J. Chem. Theory Comput.* **2010**, *6*, 2071−2085.

(98) Peach, M. J. G.; Warner, N.; Tozer, D. J. On the Triplet Instability in TDDFT. *Mol. Phys.* **2013**, *111*, 1271−1274.

DOI: 10.1021/acs.jctc.6b01169
J. Chem. Theory Comput. 2017, 13, 767−783